IN VIVO QUANTIFICATION OF GLUTAMATERGIC ABNORMALITIES IN BEHAVIORAL VARIANT FRONTOTEMPORAL DEMENTIA

Antoine Leuzy

Department of Neurology and Neurosurgery
McGill University, Montreal

December 2014

A thesis submitted to McGill University in partial fulfillment of the requirements of the degree of Masters of Science

ACKNOWLEDGMENTS

I wish to express my gratitude to my supervisor Dr. Pedro Rosa-Neto, my co-supervisor Dr. Serge Gauthier, and Dr. Jean Paul Soucy for their guidance and support throughout the duration of this project. I would also like to thank Dr. Jens Pruessner, Dr. René Désautels and Dr. Sylvain Williams.

I thank the members of the Translational Neuroimaging Laboratory, with whom I shared the last several years. In particular, I wish to thank Eduardo Rigon Zimmer, Jonathan Dubois, Maxime Parent, and Jared Rowley for their invaluable assistance throughout the data analysis phase of this project, and during the preparation of this thesis. I also wish to thank Cory Cooperman and Nida Ali.

I wish to acknowledge the help of the imaging staff at the McConnell Brain Imaging Centre, Montreal Neurological Institute, including Dr. Esther Schirmaccher, Dr. Alexey Kostikov, Reda Bouhachi, Simion Matei, and Rick Fukasawa (PET Technologists), Ron Lopez, David Costa, and Louise Marcott (MRI Technologists), and André Cormier (Chief MRI Technologist). I also wish to thank Maria Giovanna Di Nezza and Stacey Peixoto for their assistance in booking imaging slots.

I also wish to thank the research participants and their families who participated in this study, without whom the research could not progress.

I am most grateful to my family, min älskling (Kerstin Heurling) and Joshua Ejdelman for their love and support, as well as to Dr. Alan Evans, as my beginnings in his laboratory are what ultimately led me to where I am today.

FUNDING

This work was supported by the Canadian Institutes of Health Research [MOP-11-51-31 and the Frederick Banting and Charles Best Canada Graduate Scholarship], the Alan Tiffin Foundation, the Alzheimer's Association [NIRG-08-92090], and the Fonds de Recherche du Québec – Santé.

TABLE OF CONTENTS

TABLE OF CONTENTS (CONTINUED)

CONTRIBUTION OF AUTHORS

Ethics and funding: Dr. Pedro Rosa-Neto and Dr. Serge Gauthier.

Study design: Antoine Leuzy and Dr. Pedro Rosa-Neto

Cyclotron and radiochemistry: Dr. Esther Schirmaccher and Dr. Alexey Kostikov.

Data collection: Antoine Leuzy

Data analysis: Antoine Leuzy, Eduardo Rigon Zimmer and Jonathan Dubois.

Drafting of the article: Antoine Leuzy and Dr. Pedro Rosa-Neto.

Preparation of the thesis: Antoine Leuzy, Dr. Pedro Rosa-Neto, Dr. Serge Gauthier, Dr. Jean-Paul Soucy, and Dr. René Désautels.

ABSTRACT

Introduction: Although the pathogenesis underlying behavioural variant frontotemporal dementia (bvFTD) has yet to be fully understood, glutamatergic abnormalities have been hypothesized to play an important role. The aim of the present study was to determine the availability of the metabotropic glutamate receptor type 5 (mGluR5) using a novel positron emission tomography (PET) radiopharmaceutical with high selectivity for mGluR5 ([^{11}C]ABP688) in a sample of bvFTD patients. In addition, we sought to determine the overlap between availability of mGluR5 and hypometabolism, as measured using [^{18}F]FDG PET and voxel based morphometry (VBM). **Methods:** Availability of mGluR5 and glucose metabolism ([^{18}F]FDG) were measured in bvFTD (n=5) and cognitively normal (CN) subjects (n=10). [^{11}C]ABP688 binding potential maps (BP_{ND}) were calculated using the cerebellum as a reference region, with [^{18}F]FDG standardized uptake ratio maps (SUV_R) normalized to the pons. Grey matter (GM) concentrations were determined using VBM. Voxel-based group differences were obtained using RMINC. **Results:** BvFTD patients showed widespread decrements in [^{11}C]ABP688 BP_{ND} throughout frontal, temporal and subcortical areas. These areas were likewise characterized by significant hypometabolism and GM loss, with overlap between reduced [^{11}C]ABP688 BP_{ND} and hypometabolism superior to that for GM atrophy. Several regions were characterized only by decreased binding of [^{11}C]ABP688. **Conclusion:** The present findings represent the first *in vivo* report of decreased availability of mGluR5 in bvFTD. This study suggests that glutamate excitotoxicity may play a role in the pathogenesis of bvFTD and that [^{11}C]ABP688 may prove a suitable marker of glutamatergic neurotransmission *in vivo*.

RÉSUMÉ

Introduction: Bien que la pathogenèse sous-jacente à la variante comportementale de la démence fronto-temporale (vcDFT) n'ait pas encore été bien comprise, les anomalies glutamatergique ont été retenues comme ayant un rôle important dans cette équation. Le but de la présente étude était de déterminer la disponibilité du récepteur métabotropique du glutamate de type 5 (mGluR5) à l'aide d'une nouvelle tomographie par émission de positons (TEP) radiopharmaceutique possédant une haute sélectivité pour les mGluR5 ([^{11}C]ABP688) testé sur un échantillon de patients vcFDT. De plus, nous avons cherché à déterminer le chevauchement entre la disponibilité des mGluR5 et la neurodégénérescence, telle que mesurée en utilisant la base de [^{18}F]FDG et *voxel based morphométrie (VBM).* **Méthodes:** Disponibilité des mGluR5 et le métabolisme du glucose ont été mesurés dans vcDFT (n=5) et sujets normaux (SN; n=10). [^{11}C]ABP688 *binding potential maps (BP_{ND})* ont été calculées en utilisant le cervelet comme région de référence, avec [^{18}F]FDG *standardized uptake ratio maps (SUV_R)* normalisée au pons. Les concentrations de la matière grise (MG) ont été déterminées à l'aide de *VBM*. Les différences identifiées entre les groupes assujettis à voxel ont été obtenues par le biais de *RMINC*. **Résultats:** Les patients vcDFT ont montré des décroissances généralisées dans [^{11}C]ABP688 BP_{ND} dans les zones frontales, temporales et sous-corticales. Ces zones étaient également caractérisées par un hypométabolisme significatif et la perte de MG, avec un chevauchement entre la réduction [^{11}C]ABP688 BP_{ND} et un hypométabolisme supérieur à celle de l'atrophie MG. De plus, plusieurs régions ont été caractérisées uniquement par la diminution de la liaison de [^{11}C]ABP688. **Conclusion:** Les résultats actuels représentent une première dans le rapport *in vivo* de diminution de la disponibilité de mGluR5 dans vcDFT. Cette étude suggère que l'excitotoxicité

du glutamate peut jouer un rôle dans la pathogenèse de vcDFT et que [^{11}C]ABP688 peut s'avérer un marqueur approprié de neurotransmission glutamatergique *in vivo*.

CHAPTER 1: INTRODUCTION AND BACKGROUND

INTRODUCTION

Frontotemporal dementia (FTD) is the clinical diagnostic term used to describe patients presenting with a range of dementia syndromes secondary to focal neurodegeneration of the frontal and anterior temporal lobes. The spectrum of pathologies underlying these focal changes are regrouped under the heading of frontotemporal lobar degeneration (FTLD), and include the microtubule associated protein tau (MAPT), the TAR DNA binding protein of 43 kDa (TDP), and the tumor associated protein fused in sarcoma (FUS) (Mackenzie et al. 2010). In addition to the diagnostic subgroups of progressive non-fluent aphasia (PNFA) and semantic dementia (SD), FTD encompasses a behavioral variant (bvFTD), characterized by executive impairments and progressive deterioration of personality, and social function (Neary et al. 1998). Epidemiological studies suggest that FTD is the second most common cause of early onset (before 65 years of age) dementia after Alzheimer's disease (Ratnavalli et al. 2002; Rosso et al. 2003), with bvFTD representing an estimated 60% of cases (Josephs et al. 2006).

While the mechanisms of FTLD underlying bvFTD have yet to be solved, altered glutamatergic transmission is hypothesized to play a role given the selective loss of glutamatergic projection neurons in this patient population (Ferrer 1999). As the main excitatory neurotransmitter in the central nervous system, glutamate exerts its effects via ionotropic and metabotropic receptor families. In contrast to ionotropic receptors such as N-methyl-D-aspartate (NMDA)—which are coupled to ion fluxes through membrane ion channels (Bowie 2008; Lodge 2009)—metabotropic receptors are coupled via G proteins to phospholipase C activation (Masu et al. 1991). In the case of bvFTD, postmortem studies have shown declines in NMDA receptor populations within frontotemporal areas (Procter et al. 1999), suggesting that glutamate

excitotoxicity (Dodd 2002)—a detrimental scenario involving loss of cortical and subcortical neurons secondary to enhanced glutamatergic calcium signaling—may be at play, possibly in a manner similar to that seen in other neurodegenerative diseases (Rothstein 1995; Shaw 1994).

RATIONALE

Despite an evidence base suggesting glutamatergic dysfunction in bvFTD, these abnormalities have yet to be systematically characterized i*n vivo* due the absence of suitable probes for use with molecular neuroimaging. Quantification of the metabotropic glutamate receptor type (mGluR5) however, has become possible *in vivo* using [^{11}C]ABP688, a positron emission tomography (PET) radiopharmaceutical with high selectivity for mGluR5 (Ametamey et al. 2006; Ametamey et al. 2007). Recent work in the area of depression has shown [^{11}C]ABP688 to be capable of identifying reductions in mGluR5, with decreased binding found in the prefrontal cortex, cingulate, and insula, regions known to be affected in bvFTD (Deschwanden et al. 2011). Given the extensive co-localization of NMDA and mGluR5 receptors (Alagarsamy et al. 2002; Luccini et al. 2007)—as well as their physiological (Attucci et al. 2001; Benquet et al. 2002; Groveman et al. 2012) and physical links (Ango et al. 2002; Thomas 2002)—decreased binding of [^{11}C]ABP688 may reflect elevated levels of synaptic glutamate, a possible sign of early NMDA receptor mediated excitotoxicity.

RESEARCH OBJECTIVES

The overall aim of the study presented herein was to gain new insight into the potential role of mGluR5 in bvFTD. The main objectives of the study conducted were:

1) To quantify the availability of mGluR5 in bvFTD using [^{11}C]ABP688.

2) To determine the topographic overlap between [^{11}C]ABP688 findings and neurodegeneration, as measured using [^{18}F]fluorodeoxyglucose ([^{18}F]FDG) PET and voxel based morphometry (VBM).

HYPOTHESES

1) Binding of [^{11}C]ABP688 would be reduced in frontal, temporal and subcortical regions.

2) Overlap between [^{11}C]ABP688, [^{18}F]FDG and VBM would be partial.

BACKGROUND

FTD Diagnostic Criteria —Historical Aspects

In the 1980s, research groups in Lund, Sweden (Brun 1987) and Manchester, UK (Neary et al. 1988) began publishing large clinicopathological case series of patients exhibiting progressive focal degeneration of frontal and anterior temporal lobes. This new neurodegenerative entity was named FTD, with consensus based diagnostic and research criteria—specifying core diagnostic, supportive, and exclusion features—released in 1994 (Brun et al. 1994). Core affective and behavioral symptoms included loss of insight as well as personal and social awareness, disinhibition, impulsivity, stereotypies, hyperorality, and utilization behaviors. Poor performance on measures of executive functioning—in the absence of significant amnesia, aphasia, or perceptuospatial impairment—and a progressive reduction of speech were likewise consistent with a diagnosis of FTD. Though an important first attempt at defining FTD, the Lund-Manchester criteria possessed several limitations, including the absence of operational definitions and no mention of the relative importance of the various diagnostic features (Rascovsky et al. 2007).

In 1998, the Lund and Manchester criteria were further refined by Neary and colleagues (Neary et al. 1998). In addition to renaming the pathological spectrum underlying FTD as FTLD, clinical descriptions were provided for the 3 most common FTLD phenotypes: behavioral variant FTD (bvFTD), and the language variants of progressive nonfluent aphasia (PNFA) (Mesulam 1982) and semantic dementia (SD) (Hodges and Patterson 1996; Hodges et al. 1992; Snowden 1999). Further, a distinction was made between core and supportive diagnostic features, with operational definitions and occasional examples provided for each.

Recognizing that previous criteria for FTLD and associated neurobehavioral syndromes were largely designed for research purposes, McKhann and colleagues (McKhann et al. 2001) proposed a third set of criteria designed to facilitate the identification and timely referral of patients. The clinical spectrum associated with FTLD was renamed FTD, with criteria simplified into those for an insidious and progressive change in behavior and those for gradual and progressive changes in language function, effectively collapsing PNFA and SD into a progressive aphasic category. Though a useful heuristic on clinical grounds, the McKhann criteria lacked the specificity required for research purposes (Rascovsky et al. 2007).

Limitations of the Neary Criteria for bvFTD and the Revised FTDC Criteria

Despite their widespread acceptance and use in both research and clinical practice, several limitations characterize the Neary Criteria. Among them, the large number of features, making routine application in clinical settings problematic, as well as the use of ambiguous descriptors and the lack of a probabilistic framework with respect to diagnostic certainty (Rascovsky et al. 2007). Moreover, a number of studies have shown their relative restrictiveness early on the disease course, an important limitation given that disease-modifying treatments are likely to be most effective in the early stages of bvFTD (Mendez et al. 2007; Piguet et al. 2009; Rascovsky et al. 2007).

In an effort to address the limitations of the 1998 criteria and to incorporate advances in the characterization and diagnosis of bvFTD, the International bvFTD Criteria Consortium (FTDC) was formed, and tasked with the development of revised diagnostic guidelines. In contrast to earlier guidelines, the FTDC criteria are hierarchical, incorporating levels of diagnostic certainty (Rascovsky et al. 2011). A diagnosis of possible bvFTD is made on clinical

grounds alone, requiring three of six behavioral/cognitive symptoms, including behavioral disinhibition, apathy or inertia, loss of empathy, perseverative, stereotyped or compulsive/ritualistic behavior, hyperorality and a neuropsychological profile showing executive deficits with relative preservation of memory and visuospatial functions. The flexibility of this classification scheme allows for variability of symptom presentation at onset, with the attendant aim of identifying patients at the mildest stages of disease. In addition to meeting criteria for possible bvFTD, significant functional decline and supportive imaging results are required for the diagnosis of probable bvFTD. Finally, the classification of bvFTD with definite FTLD pathology is limited to patients who, in addition to meeting criteria for possible or probable bvFTD, have histopathological evidence of FTLD at biopsy or post-mortem, or harbor a known pathogenic mutation. In a large multicentric study, these criteria proved more sensitive than the Neary criteria—86% versus 53%—in a sample of pathologically verified bvFTD (Rascovsky et al. 2011), though prospective studies addressing the reliability and specificity of these revised guidelines have yet to be conducted.

Epidemiology

Of the different clinical FTD syndromes, the behavioral variant is the most common, accounting for approximately 60% of cases (Josephs et al. 2006). The small number of studies and the inclusion of language variants, however, complicate the accurate ascertainment of bvFTD prevalence. Estimates from the three studies that focused on bvFTD, however, ranged from 2 to 15.4 per 100 000 persons in the 45 to 64 year age range (Harvey et al. 2003; Ikejima et al. 2009; Rosso et al. 2003). The low estimates of prevalence reported in two of these studies are likely

due the use of the 1994 Lund and Manchester Groups criteria (Brun et al. 1994), which are known to possess relatively poor sensitivity (Rascovsky et al. 2007).

Though several studies have reported disease onset in older age (Johnson et al. 2005; Shinagawa et al. 2008)—including 3% in 85 year olds (Gislason et al. 2003)—onset is typically below age 65 (Boronni et al. 2008). With respect to sex distribution, several large studies have reported a male preponderance (Hodges et al. 2003; Rascovsky et al. 2011), however other studies reported no differences (Rascovsky et al. 2005; Roberson et al. 2005; Ratnavalli et al. 2002). Studies of survival in pathologically confirmed cases of bvFTD report median survival times of 8.7 and 9.9 years from diagnosis (Roberson et al. 2005; Chiu et al. 2010), in line with the average of 7.8 years reported in a recent study using autopsy confirmed cases of bvFTD (Rascovsky et al. 2011). Overall, bvFTD is associated with shorter survival and more rapid cognitive and functional decline relative to both additional FTD subtypes and AD (Rascovsky et al. 2005; Roberson et al. 2005).

Clinical Features

The initial symptoms of bvFTD are typically behavioral and personality based, with patients often exhibiting an admixture of apathy and disinhibition (Swartz et al. 1997). Apathy follows loss of integrity in dorsomedial prefrontal structures, and manifests as passivity, social disengagement, a lack of interest in personal affairs, and neglect of personal hygiene (Rabinovici et al. 2008). Disinhibition follows dysfunction within orbital and ventromedial prefrontal areas, and is characterized by an affective shift toward inappropriate joviality, a range of impulsive behaviors including economic extravagances, sexually and socially inappropriate behaviors, verbal dysdecorum (Neary et al. 1998), psychomotor hyperactivity and, more rarely, sociopathic

acts (Mendez et al. 2005). Infrequently, presenting features can include new onset ludomania and the tetrad of hyper-religiosity, hypergraphia, hyposexuality, and viscosity characteristic of Geshwind syndrome (Manes et al. 2010; Postiglione et al. 2008). While all neuropsychiatric features found in bvFTD can occur in other dementias, their early emergence and predominance throughout the disease course typify bvFTD. Stereotyped behaviors are apparent in a majority of patients, and range from repetitive motor behaviors—such as picking, hand rubbing, clapping, and rocking (Mendez et al. 2005)—to more complex compulsions including checking, cleaning, wandering a fixed route, and idiosyncratic hoarding (Mendez et al. 2008; Perry and Miller, 2001). Compulsive self-injurious behavior has also been reported in the form of trichotillomania, picking at fingers to the point of excoriation, and self-biting (Mendez et al. 1997; Passant et al. 2005). In addition, changes in eating behavior are frequent, encompassing overeating despite endorsing satiety, overfilling of the mouth, and idiosyncratic food fads (Woolley et al. 2007). Hyperorality is also frequent, and may include excessive drinking, gum chewing, alcohol and/or tobacco consumption (Gustafson 1987). In a minority of patients with more advanced bvFTD, hyperorality may manifest as the mouthing of non-food items and consumption of inedible objects (Gustafson et al. 1992; Mendez and Foti 1997b).

Social cognition is severely affected in bvFTD. Invariably, patients lose the ability to adopt the perspectives of others, displaying a lack of concern for the implications of their behavior, alongside emotional shallowness and loss of warmth (Gregory and Hodges, 1996; Neary et al. 1998; Rankin et al. 2005). While loss of insight is common at presentation, its presence is not universal (Evers et al. 2007) with reports of both relative preservation and a wide range of impairment on Frontal Behavioral Inventory (FBI) discrepancy scores tied to symptom presence and severity (Banks and Weintraub 2009). More recent work, moreover, suggest that

the loss of insight frequently seen in bvFTD is perhaps more accurately described as indifference or anosodiaphoria rather than anosognosia (Mendez et al. 2008). Considered a core feature in the 1998 diagnostic criteria—alongside insidious onset, gradual progression, and impairment in regulation of personal conduct—loss of insight has been omitted from the recently proposed International Criteria (Rascovsky et al. 2011) on the grounds that its continued inclusion may result in suboptimal discrimination due the fact that its presence is common across numerous neurodegenerative diseases, including AD (Rascovsky et al. 2007).

Nonprogressive bvFTD: bvFTD 'phenocopies'

Recent studies have identified a subset of patients referred to as bvFTD 'phenocopies' owing to the presence of behavioral features characteristic of bvFTD in the absence of brain atrophy or hypometabolism at baseline (Kipps et al. 2009; Kipps et al. 2007). Further, they do not exhibit progressive volume loss, leading some authors to suggest that the syndrome is not due an underlying neurodegenerative etiology. Owing to the near normal life expectancy of these patients, large pathological series have yet to become available, with FTLD pathology absent among the few cases that have examined postmortem (Kipps et al. 2010). As such, the neuropathological correlates of these patients remain unclear.

While being indistinguishable from progressive bvFTD behaviorally, phenocopy cases have been identified on the basis of differential performance on activities of daily living (ADL) tasks. Though phenocopy and progressive bvFTD patients did not differ on the caregiver-based Disability Assessment of Dementia (DAD) scale, progressive patients scored significantly lower on the performance-based Assessment of Motor and Process Skills (AMPS) (Mioshi et al. 2009).

Although the AMPS discriminated well between the two groups, a grounded theory derived qualitative rating developed to evaluated the assessment session resulted in better discrimination, and correlated well with MRI ratings (Mioshi et al. 2009b). In a follow up study, only those with significantly impaired DAD total scores were found to exhibit functional decline within a 12-month period despite similar levels of impairment at baseline (Mioshi and Hodges 2009b).

Using neuropsychological measures of executive functioning, the performance of phenocopies was found to be in the normal range across the majority of tasks (Hornberger et al. 2008), with global cognitive screening measures likewise paralleling those of controls (Kipps et al. 2008). Of note, however, is the finding that up to 25% of patients with progressive bvFTD proved normal in terms of their performance on neuropsychological measures at presentation (Hornberger et al. 2008), suggesting that normal scores on neuropsychological measures alone cannot be deemed a reliable exclusion criteria, and that such measures should be corroborated when possible by neuroimaging and/or ADL measures. Performance in the area of social cognition has likewise been identified as a potential discriminator owing to the well-established impairment of bvFTD patients in such areas as Theory of Mind (Lough et al. 2006; Sturm et al. 2008). At present, however, the value of everyday application of such tests in clinical practice remains untested owing to the absence of normative age-related data.

Though the etiology of phenocopy cases remains unknown, it has been suggested that the changes seen in these patients may not be due an underlying neurodegenerative process. Given the important overlap between many of the features of bvFTD and those seen in neuropsychiatric conditions, some authors have proposed that the majority of phenocopy cases tend to be atypical presentations of psychiatric disorders, including late onset bipolar disorder, atypical depression, alcohol abuse, and chronic attention-deficit hyperactivity disorder (Manes 2012; Manes et al.

2010). Additional suggestions include decompensated personality disorders or autism spectrum disorders such as Asperger's syndrome manifest at a level below that required for formal psychiatric diagnosis (Kipps et al. 2010). An additional hypothesis recently emerged from work by Khan and colleagues who reported two bvFTD cases characterized by very subtle atrophy, a relatively stable clinical course, and *C9ORF72* hexanucleotide expansions (Khan et al. 2012). This finding may suggest that some phenocopy patients have a more indolent form of bvFTD with TDP-43 pathology.

Neuropathology

The FTLDs comprise a heterogeneous group of diseases that share the finding of bilateral frontotemporal atrophy, microvacuolation, and, to a variable degree, astrocytic gliosis (Piguet et al. 2011). Each disease, however, differs with respect to biochemical signature, comprising inclusion composition, morphology, and distribution (Cairns et al. 2007). In this respect, the microtubule associated protein tau (MAPT) (Hutton et al. 1998), the transactive response DNA binding protein of 43 kD (TDP-43) (Arai et al. 2006; Neumann et al. 2006), and the tumor associated protein fused in sarcoma (FUS) (Kwiatkowski et al. 2009) have been identified as key molecular players underlying neurodegeneration seen in FTLD. Virtually all cases of FTLD can therefore be classified into FTLD-tau, FTLD-TDP, or TDP-FUS, with further subclassification on the basis of inclusion morphology/ lesion distribution (Cairns et al. 2007; Mackenzie et al. 2010; Mackenzie et al. 2009) and—in the case of FTLD-tau—the relative predominance of three or four microtubule binding repeats (Cairns et al. 2007). A fourth category—FTLD-other—is reserved for cases with immunohistochemistry against proteins of the ubiquitin proteosomal system or cases for which the major protein remains unknown (Mackenzie et al. 2010).

In contrast to the progressive aphasic syndromes, which typically exhibit greater association with one histological variant of FTLD over another (PNDA with FTLD-tau and SD with FTLD-TDP (Piguet et al. 2011), bvFTD can be associated with all histological variants of FTLD (Josephs et al. 2006b; Hodges et al. 2004; Kertesz et al. 2005). Cases, however, are generally split approximately 50:50 between FTLD-tau and TDP (Hodges et al. 2004; Shi et al. 2005; Snowden et al. 2007), with a small proportion of cases accounted for by FTLD-FUS (Seelaar et al. 2010). In addition, on the basis of recent clinicopathological studies, some investigators have proposed more specific links between apparent bvFTD sub-types and specific molecular pathologies. For instance, FTLD-FUS has been tightly linked to a form of bvFTD characterized by striatal pathology, youthful onset, prominent stereotypies, hypersexuality, and hyperphagia (Snowden et al. 2011), a finding that links previous reports of marked striatal atrophy in patients with bvFTD and stereotypy (Josephs et al. 2008) and striking striatal atrophy in FTLD-FUS (Josephs et al. 2010). The general absence, however, of strong ties between bvFTD and any of type FTLD subtype, has led some to question whether the syndrome of bvFTD needs to be revised (Josephs et al. 2011).

Genetics

Approximately 50% of bvFTD patients have a family history of dementia (Rohrer et al. 2009), with an autosomal dominant pattern of inheritance noted in 10 to 30% of pedigrees (Goldman et al. 2005; Seelaar et al. 2008). To date, mutations in seven genes have been association with bvFTD, including progranulin *(GRN)* (Baker et al. 2006; Cruts et al. 2006), the microtubule associated protein tau *(MPAT)* (Gass et al. 2006; Hutton et al. 1998), valosin-containing protein *(VCP)* (Neumann et al. 2007; Forman et al. 2006; Watts et al. 2004), chromatin-modifying

protein 2B *(CHMP2B)* (Skibinski et al. 2005), transactive response DNA-binding protein *(TARDBP)* (Sreedharan et al. 2008), fused in sarcoma *(FUS)* (Kwiatkowski et al. 2009; Vance et al. 2009), and the C9 opening reading frame 72 *(C9ORF72)* (DeJesus-Hernandez et al. 2012; Renton et al. 2011) (for review, see Sieben et al. 2012). While mutations in *MAPT* and *GRN* genes are thought to account for 10 to 20% of familial cases, *C9ORF72* mutations are now believed to be the most common genetic abnormalities in familial bvFTD (Riedl et al. 2014). On pathological grounds, both *C9ORF72* and *GRN* mutations are associated with deposition of the transactive response DNA binding protein of 43 kDa *(TDP-43),* while mutations in *MAPT* are associated with deposition of hyperphosphorylated tau (Josephs et al. 2011).

Structural Imaging

As a syndromic entity bvFTD has classically been viewed as a result of atrophy within the frontal cortices, typically symmetric, though right-sided asymmetry has been reported (Fukui and Kertesz 2000; Rosen et al. 2002; Seeley et al. 2008). More recent studies, however, highlight involvement of rostral limbic areas, including the anterior cingulate, anterior insula, limbic ventral striatum, amygdalae, periaqueductal gray, (Barnes et al. 2006; Boccardi et al. 2005; Rosen et al. 2002; Whitwell et al. 2005) as well as temporal lobe structures such as the hippocampus and parahippocampal gyri (Barnes et al. 2006; Galton et al. 2001; Whitwell et al. 2009). VBM studies have leant support to the concept of bvFTD as a fronto-striatal disorder (Looi et al. 2012), on the basis of gray matter volume reduction in the anterior medial frontal cortex, dorsolateral prefrontal cortex, and anterior cingulate, extending to the insular cortex, and subcortical striatal regions (Pan et al. 2012). VBM studies have, furthermore, helped delineate four anatomical subtypes, with two of these of these subtypes exhibiting predominant gray

matter volume loss in the temporal lobe (temporal-dominant, temporoparietal dominant), with gray matter volume loss in the remaining two subtypes predominant in the frontal lobes (frontal dominant, frontotemporal dominant). Importantly, subtypes differed on measures of confrontation naming, episodic memory, and executive function, though not in terms of behavioral severity (Whitwell et al. 2009b).

Using deformation-based morphometry, Cardenas et al. confirmed frontal and anterior temporal lobe atrophy in bvFTD, and, in addition, reported significant atrophy in the pons, midbrain, inferior/superior colliculus, and the thalamus (Cardenas et al. 2007). Atrophy has, moreover, been found to vary as a function of behavioral profile (Cummings 1993; Hodges 2001; Josephs et al. 2006c Le Ber et al. 2006; Liu et al. 2004; Massimo et al. 2009; Snowden et al. 2001; Whitwell et al. 2006). Specifically, apathetic patients have been shown to exhibit greater atrophy within dorsolateral and medial frontal cortices, with disinhibited patients exhibiting greater atrophy within medial orbitofrontal cortices and temporal lobe (Le Ber et al. 2006; Massimo et al. 2009). Recent clinicopathological studies have identified an additional subtype characterized by prominent stereotypy associated with marked striatal atrophy (Josephs et al. 2008).

Functional Imaging

Functional imaging in bvFTD using [^{18}F]FDG has shown significant hypometabolism in superior, middle, and prefrontal gyri, orbitofrontal and medial frontal areas, as well as the cingulate gyri. Hypometabolism was also noted in the anterior/ventral temporal lobe, the left inferior parietal lobule, the insula, the uncus, right cerebellar tonsil, and in subcortical structures including the putamen, globus pallidus, dorsomedial thalamus, hypothalamus, and pulvinar (Jeong et al. 2005).

In line with previous findings (Grimmer et al. 2004; Kamo et al. 1987) metabolic declines in bvFTD, while predominant in frontal, anterior temporal, and subcortical structures, are more widespread than previously recognized (Ishii et al. 1998). Moreover, subtype specific metabolic signatures have been identified, with the apathetic subtype associated with hypometabolism predominantly in the dorsolateral prefrontal cortex, and the disinhibited subtype associated with marked metabolic reductions in limbic structures including the cingulate cortex, hippocampus/amygdala, and nucleus accumbens (Franceschi et al. 2005).

Studies using ^{99m}Tc-ECD SPECT have revealed considerable anterior hypoperfusion, particularly affecting the frontal cortex, anterior cingulate, anterior temporal cortex, and parahippocampi and hippocampi, with relative sparing of the posterior cingulate, as well as of the parietal and occipital cortices (Basely et al. 2013). Importantly, relative to AD, bvFTD patients showed greater declines in regional cerebral blood flow in medial temporal lobe (MTL) structures, though characterized by a more anterior/parahippocampal topography. Both global and MTL specific findings are in line with findings from studies using ^{99m}Tc-HMPAO SPECT (Neary et al. 1987; Talbot et al. 1998; Varma et al. 2002).

Neuroreceptor Imaging

Postmortem studies of FTLD patients point to dysfunction of the serotonergic system, with significant neuronal loss in the nucleus centralis superior and nucleus raphe dorsalis, suggesting involvement of ascending serotonergic projection fibers (Yang and Schmitt 2001). Furthermore, a significant loss of serotonergic receptors was observed in frontal and temporal cortices of post-mortem brain tissue sections from FTLD patients (Procter et al. 1999). PET imaging using [^{11}C]MDL revealed a marked reduction of $5HT_{2A}$ receptors in orbitofrontal, medial frontal and

cingulate cortices, as well as in the mesencephalon, the latter finding supporting the hypothesis of involvement of the ascending serotonergic system (Franceschi et al. 2005*)*.

Extrapyramidal deficits have been observed in bvFTD following neurodegeneration of the basal ganglia, (Brun and Passant 1996) substantia nigra and locus ceruleus (Mann et al. 1993). Using [^{11}C]CFT PET, presynaptic dopaminergic function within the nigrostriatal system has been shown to be reduced in bvFTD, with decreased binding in both the caudate and putamen, a finding related to severity of extrapyramidal symptomatology (Rinne et al. 2002). Similar findings were obtained using ^{123}I-FP-CIT SPECT, with motor UPDRS scores shown to correlate negatively with ^{123}I-FP-CIT uptake (Sedaghat et al. 2007). Moreover, in a family with FTD and parkinsonism linked to chromosome 17 (FTDP-17), presynaptic dopaminergic deficits within the striatum were demonstrated using SPECT and a tropane derivative targeting the dopamine transporter (Sperfeld et al. 1999).

Amyloid PET Imaging

While cerebral amyloidosis is not a characteristic neuropathological feature of bvFTD many patients with pathologically verified FTLD have dementia due to AD as antemortem clinical diagnosis. Moreover, 10-40% of patients diagnosed with FTLD are found to have AD postmortem (Alladi et al. 2007; Varma et al. 1999). Accurate diagnosis can prove challenging given common clinical features (Galton et al. 2000; Graham et al. 2005) and increasingly apparent anatomic overlap of supposedly distinct topographic signatures of atrophy and metabolic decline, as revealed by MRI and FDG-PET (Foster et al. 2007; Rabinovici et al. 2007b; Womack et al. 2011).

In small scale studies conducted to date, molecular imaging of amyloid is nevertheless

apparently useful in differentiating FTLD from AD (Engler et al. 2008; Rabinovici et al. 2007; Rowe et al. 2007), with the majority of FTD patients showing no retention of [^{11}C]PIB or [^{18}F]AV45 (Vardy et al. 2010). Few in number, reports of amyloid-positive FTLD cases may represent false positives, comorbid FTLD/AD pathology, or the frontal variant of AD (Rabinovici et al. 2007).

Glutamatergic neurotransmission, and the excitotoxicity hypothesis

As the principle excitatory neurotransmitter in the human central nervous system, glutamate is involved in the regulation of virtually all aspects of cognition, perception, and behavior (Schaeffer and Duplantier 2010). Following its synthesis from glutamine in the synaptic nerve terminal, glutamate is translocated into synaptic vesicles via the action of vesicular glutamate transporters (Liguz-Lecznar and Skangiel-Kramska 2007), and released into the synaptic cleft in response to an action potential. Synaptic clearance of glutamate is mediated by a family of excitatory amino acid transporters, expressed predominantly on astrocytes (Bunch et al. 2009). Following astrocytic reuptake, glutamate is converted to glutamine and stored until additional levels of glutamate are required.

Glutamate signaling is mediated through two major receptor families, ionotropic and metabotropic. Directly coupled to membrane ion channels, ionotropic receptors (iGluRs) are predominantly expressed post-synaptically and include NMDA, (3-hydroxy-5-methylisoxazol-4-yl) propionic acid (AMPA) and kainate (KA) (Dingledine et al. 1999). The metabotropic glutamate receptors (mGluRs) comprise a family of eight G-protein coupled receptor subtypes, and can be divided into three groups on the basis of sequence homology, ligand binding, and G-protein coupling specificity. Group I receptors (mGluR 1 and 5) are typically localized post-

synaptically, and activate the phospholipase C pathway via Gq signaling (Karim et al. 2001; Warwick et al. 2005), Group II (mGluR 2 and 3) and III (mGluR 4, 6, 7, and 8) receptors are preferentially located pre-synaptically, and couple to Gi/Go, signaling via inhibition of adenylate cyclase (Pin and Duvoisin 1995; Conn and Pin 1997; Harrison et al. 2008). In contrast to iGluRs—which are involved primarily in fast synaptic transmission—mGluRs generally exert a neuromodulatory role, mediating slower responses to synaptic glutamate, in keeping with their second messenger signaling mechanism (Niswender and Conn 2010).

While a tightly regulated process under normal physiological conditions, various pathophysiological conditions are capable of disrupting glutamatergic signaling, resulting in excessive levels of extracellular glutamate. The concept of neuronal degeneration due the resulting over-stimulation of glutamate receptors—the so-called excitotoxicity hypothesis—was first formulated by Olney (Olney 1978) and is well supported experimentally, both *in vitro* and *in vivo* (Doble 1999). In contrast to classical excitotoxicity—where neuronal damage is induced by acute elevation of glutamate, such as in cerebral ischemia and neurotrama—milder, more chronic elevations of glutamate are believed to be at play in the case of neurodegenerative diseases (Doble 1999). In this scenario, despite normal levels of synaptic glutamate, weakened postsynaptic neurons become sensitized to glutamate stimulation, resulting in elevated levels of intracellular levels of Ca^{2+} and resulting neuronal death. In both forms of excitotoxicity, however, the NMDA receptor is believed to be the primary mediator of Ca^{2+} related neuronal injury, with this mechanism of neuronal damage appearing to be involved in a wide range of neurodegenerative diseases (for review, see Kalia et al. 2008). Importantly, mGluR5 has emerged as an attractive therapeutic target given its ability to modulate NMDA receptor currents (Alagarsamy et al. 1999).

Structure, Function, and Regional Expression of MGluR5

MGlu5 receptors possess a large extracellular N-terminal domain and seven transmembrane (7TM) spanning regions interjoined by three intracellular/extracellular loops (Spooren et al. 2003). The N-terminal domain is bi-lobed in structure, with the lobes separated from the transmembrane region of the receptor by a cysteine-rich region, forming a cavity where glutamate binds (Costantino et al. 2001; Costantino and Pellicciari, 1996). Upon binding of glutamate to its orthosteric site, the lobes enclose the crevice, with glutamate thought to provide conformational stability via the generation of bonds with residues of both lobes (Bessis et al. 2000; Kunishima et al. 2000). In addition to this 'Venus flytrap' mechanism of receptor activation, the cysteine-rich region is though to constitute a flexible spacer, allowing mobilization of the glutamate binding site towards the transmembrane domains (Hermans et al. 2001). Importantly, mGlu5 receptors can assume distinct homooligomeric or heteromeric conformations—usually as disulfide-linked dimers—that seems to be very sensitive to glutamate binding to the orthosteric site (Romano et al. 1996; Cabello et al. 2009). More specifically, glutamate binding seems to stabilize and change the orientation of mGlu5 extracellular domain. As a consequence, the C-terminal part of the extracellular domain, moves closer, which seems to trigger the switch to dimeric states. (Kunishima et al. 2000).

MGluR5 expression levels are moderate in the olfactory tubercle, the anterior olfactory nucleus as well as in the main and accessory bulb. Moderate to high receptor densities characterize the limbic and neocortex (layers I-VI), including the subiculum, entorhinal, cingulate, and piriform cortical regions (Romano et al. 1995). Within the amygdala, moderate receptor levels are found, with high expression levels in basal ganglia input regions (nucleus accumbens and striatum) and moderate levels in output regions (globus pallidus, substantia nigra,

subthalamic nucleus). The hippocampus shows high receptor levels in the cornu ammonis subfields 1 and 3, as well as in the molecular layer and hilus of the dentate gyrus. With the exception of the lateral septal nucleus, the septum and basal forebrain exhibit relatively low expression levels of mGluR5, as do the thalamus, hypothalamus, midbrain, and cerebellum (Romano et al. 1995).

Quantification of mGluR5 using [^{11}C]ABP688 PET

The discovery of non-amino-acid molecules with high selectivity and affinity for the mGluR5 transmembrane allosteric binding site has led to advances in our ability to quantify mGluR5 density. In this respect, the radiopharmaceutical 3-(6-methyl-pyridin-2-ylethynyl)- cyclohex-2-enone-O-11C-methyloxime ([^{11}C]ABP688) has been developed for assessment of mGluR5 availability *in vivo* using PET imaging (Ametamey et al. 2006). A negative allosteric modulator for mGluR5, [^{11}C]ABP688 exhibits high selectivity and favorable kinetics. After intravenous administration, [^{11}C]ABP688 distributes to various organs, in particular the liver, gall bladder and kidneys, following fast liver metabolism (Treyer et al. 2008; Treyer et al. 2007). Due to its optimal lipophilicity (logD=2.4), [^{11}C]ABP688 easily crosses the blood brain barrier (BBB; fist pass extraction fraction > 0.9) and binds with high affinity (K_d=1.7 ± 0.2 nM) to mGLUR$_5$ (Treyer et al. 2008). Moreover, [^{11}C]ABP688 metabolites are hydrophilic and do not cross the BBB, and therefore do not contribute to brain activity.

Previous *in vivo* studies of [^{11}C]ABP688 PET in healthy subjects showed high binding in known mGluR5 dense regions such as the striatum, the hippocampus, and the anterior cingulate cortex (Ametamey et al. 2007; Treyer et al. 2007). While preliminary kinetic analysis using arterial input function (gold standard method) indicates that [^{11}C]ABP688 binding is better

described by a 2-tissue compartment model (Ametamey et al. 2007b), simplified reference tissue models have been shown to be suitable for *in vivo* quantification using PET owing to negligible binding in the cerebellum (Elmenhorst et al. 2010). The [^{11}C]ABP688 imaging outcome described in chapter 2 is the non-displaceable binding potential (BP_{ND}), which simultaneously reflects the availability and affinity of $mGLUR_5$ binding sites for [^{11}C]ABP688. It is an "equivalent" *in vivo* measure of the autoradiography single dose experiment parameter B_{max}/K_d.

Quantification using PET and the Simplified Reference Tissue Method

In vivo quantification of radioligand-receptor binding using PET requires the estimation of tracer uptake, washout, retention in tissue as a function of time (tissue response function), and tissue delivery (arterial input function). In order to obtain measurements of plasma tracer levels in arterial blood, arterial cannulation is required. For a majority of receptor radioligands, however, total plasma concentration measurements are insufficient, with the determination of the fraction of labelled metabolites over time an additional requirement (Lammertsma and Hume 1996). In addition, though arterial blood sampling has been shown to be safe in research subjects (Everett et al. 2009), the invasiveness and complexity of this method renders it unsuitable for routine use in certain patient populations.

In order to circumvent the complexities of arterial input function, a reference tissue model was developed (Lammertsma et al. 1996b; Hume et al. 1992) in which arterial plasma sampling is replaced by the time-activity curve of a reference regions exhibiting negligible specific uptake of the radiotracer in question. This original simplified model fit four parameters. Though estimation of the parameter of interest (binding potential; BP) proved robust, estimates of the remaining parameters—including the plasma to tissue transfer rate—proved imprecise, with slow

convergence rates (Lammertsma and Hume 1996). As such, a three-parameter model was developed (Lammertsma and Hume 1996), which, in addition to yielding BP values essentially the same as those obtained using the four-parameter model, is characterized by rapid convergence and greater stability for remaining parameters (Lammertsma and Hume 1996). Following this, the simplified reference tissue method has been implemented at the voxel level to produce parametric BP images using a basis functions approach (Gunn et al. 1997).

Voxel Based Morphometry

In contrast to traditional techniques for the assessment of atrophy using MRI—which include expert based visual assessment and manual delineation of regions of interest—automated techniques allow for the analysis of atrophy across large groups of individuals without the need for subjective visual ratings and laborious manual tracings. VBM is one such technique, and has proved quite popular since its introduction (Wright et al. 1995; Ashburner and Friston, 2000), given that it is relatively easy to use and has provided biologically plausible results (Whitwell and Josephs 2007; Whitwell and Jack 2005b). Typically using T1-weighted volumetric MRI images, VBM identifies differences in the relative concentration of gray or white matter, while controlling for large-scale differences in gross anatomy. Regional differences in the volume of gray or white matter can likewise be determined through the use of a further processing step know as "modulation" (Good et al. 2001). Finally, regression analysis can be used at the voxel level to determine neuroanatomical correlates of clinical features of interest (Whitwell 2009).

Following spatial normalization—generally achieved using a two-step approach comprising a 12-parameter affine transformation followed by a nonlinear registration using a mean squared difference matching function (Ashburner and Friston, 2000)—images are

segmented in gray matter (GM), white matter (WM), and cerebrospinal fluid (CSF). Typically, analysis is performed on GM, though WM can also be analyzed, depending on the question of interest. Resulting images are then smoothed, with the dimensions of the smoothing kernel determining the number of voxels averaged at each point (Karas et al. 2003; Whitwell et al. 2009b). In addition to increasing data conformity with respect to the Gaussian field model, smoothing reduces intersubject variability, increasing the validity of parametric tests (Ashburner and Friston, 2000; Salmond et al. 2002). Smoothing likewise increase the sensitivity to detect group differences, though excessive smoothing decreases spatial resolution.

Once the segmented images have been smoothed, parametric statistical analysis is carried out using the general linear model, with the null hypothesis assuming no between group differences. The theory of Gaussian random fields applied to determine significance (Ashburner and Friston, 2000), followed by correction for multiple comparisons to reduce the risk of false-positive error, typically using the family-wise error (FWE) correction (Friston et al. 1993), or the more lenient false discovery rate (FDR) correction (Genovese et al. 2002). Though VBM findings often prove difficult to validate, studies addressing correspondence between VBM analyses and traditional measurement techniques—including manual volumetry—have shown relatively good agreement (Good et al. 2002; Giuliani et al. 2005; Whitwell et al. 2005c; Davies et al. 2009, Focke et al. 2014), lending support to the biological validity of VBM.

CHAPTER 2: RESEARCH MANUSCRIPT

In vivo characterization of metabotropic glutamate receptor type five abnormalities in behavioural variant FTD

Antoine Leuzy[a,b], Eduardo Rigon Zimmer[a,b,c], Jonathan Dubois[d], Jean-Paul Soucy[e], Alexey Kostikov[e], Esther Schirmaccher[e], René Désautels[f], Serge Gauthier[b], and Pedro Rosa-Neto[a,b*]

[a]*Translational Neuroimaging Laboratory, Douglas Mental Health University Institute, Montreal, Canada*
[b]*Alzheimer's Disease Research Unit, McGill Centre for Studies in Aging, McGill University, Montreal, Canada*
[c]*Department of Biochemistry, Federal University of Rio Grande do Sul, Porto Alegre, Brazil*
[d]*Department of Neurology and Neurosurgery, Montreal Neurological Institute , Montreal, Canada*
[e]*McConnell Brain Imaging Centre, Montreal Neurological Institute, Montreal, Canada*
[f]*Geriatric Psychiatry Program, Douglas Mental Health University Institute*

[*]**Correspondence to:** Dr. Pedro Rosa-Neto
McGill Center for Studies in Aging
6825 LaSalle Blvd. Montreal, QC, Canada H4H 1R3
E-mail: pedro.rosa@mcgill.ca
Tel.: (+1) 514-761-6131 (ext. 6310)
Fax.: (+1) 514-888-4050

Keywords: Behavioural variant frontotemporal dementia, Frontotemporal lobar degeneration, Positron Emission Tomography, 11C-ABP688, Metabotropic glutamate receptor type 5, Excitotoxicity

Submitted to *Brain Structure and Function* on August 14, 2014.

Introduction

Behavioural variant frontotemporal dementia (bvFTD) is a progressive neurodegenerative syndrome characterized by change in personality, social cognition impairment, and executive dysfunction (Mendez et al. 2008; Swartz et al. 1997). Approaching Alzheimer's disease (AD) as the leading cause of early-onset (before 65 years of age) dementia (Ratnavalli et al. 2002; Rosso et al. 2003), bvFTD arises from a heterogeneous range of pathologies—referred to collectively as frontotemporal lobar degeneration (FTLD)—resulting in degenerative changes within frontal paralimbic, temporal and subcortical brain regions. In most cases, patients show either deposition of the microtubule associated protein tau (tau) or the TAR DNA binding protein of 43 kDa (TDP) (Mackenzie et al. 2010). A minority, however, show a defect in metabolism of the tumor associated protein fused in sarcoma (FUS). The majority of FTLDs can therefore be classified into FTLD-tau, FTLD-TDP, or FTLD-FUS, with further subclassification based predominantly on inclusion morphology and lesion distribution (Mackenzie et al. 2010).

Although the pathogenic mechanisms underlying bvFTD have yet to be fully elucidated, aberrant glutamatergic neurotransmission has been hypothesized to play a role. The primary excitatory neurotransmitter in the mammalian brain, glutamate acts via ionotropic and metabotropic receptors (Schaeffer and Duplantier 2010). Whereas ionotropic receptors mediate fast excitatory neurotransmission, metabotropic glutamate receptors (mGluRs) play an important role in synaptic modulation via regulation of neuronal excitability, transmitter release, synaptic plasticity and glial function. In the case of bvFTD, FTLD has been found to accumulate preferentially within paralimbic and homotypical heteromodal brain regions, areas rich in excitatory glutamatergic pyramidal cells. Indeed, several autoradiographic and immunohistochemical studies in post-mortem bvFTD tissue have provided evidence supporting this hypothesis (Dalfo et al. 2005; Ferrer 1999; Procter et al. 1999), highlighting reduced expression of the N-methyl-D-aspartate (NMDA) ionotropic glutamate receptor. Importantly, activation of mGluR5 was shown to regulate glutamatergic neurotransmission via modulation of NMDA receptor functionality (Llansola and Felipo 2010; Niswender and Conn 2010; Perroy et al. 2008). Moreover, mGluR5 signaling has been shown to be critically involved in the normal cognitive functioning of various neuronal

populations (Schaeffer and Duplantier 2010), including those within FTLD predilection sites (Ferraguti and Shigemoto 2006).

Despite a strong *in vitro* evidence base, glutamatergic abnormalities in bvFTD have yet to be systematically characterized i*n vivo* owing to the lack of suitable molecular probes. Using [^{11}C]ABP688—a novel Positron Emission Tomography (PET) radiopharmaceutical with high selectivity for mGluR5 (Ametamey et al. 2006; Ametamey et al. 2007)—we sought to measure mGluR5 availability and to determine the topographic overlap with neurodegeneration within frontotemporal and subcortical brain regions, as indexed using [^{18}F]fluorodeoxyglucose ([^{18}F]FDG)-PET and voxel based morphometry (VBM).

Methods

Subjects

Five patients meeting research criteria for probable bvFTD (Rascovsky et al. 2011) were recruited from the McGill Centre for Studies in Aging (MCSA) Alzheimer's Disease Research Unit. Exclusion criteria were (i) past or present use of memantine; (ii) presence of other neurological diseases; (iii) premorbid psychiatric disease or intellectual disability; (iv) history of head injuries and loss of consciousness following head trauma; (v) current (within 1 month) use of psychoactive substances; (vi) parkinsonism—as identified using the United Parkinson's Disease Rating Scale (Goetz et al. 2007)—(vii) the presence of any major structural anomaly or signs of major vascular pathology on MRI evaluation (Roman et al. 1993); or the presence of amyloid pathology—as indexed using carbon-11 Pittsburgh Compound B ([^{11}C]PIB) PET—given that bvFTD and the frontal variant of AD are often difficult to differentiate on clinical grounds alone (Alladi et al. 2007). The diagnosis of bvFTD was determined during a multidisciplinary conference taking into consideration available medical, imaging, and complementary laboratory information.

The bvFTD subjects were matched by age and gender to a group of 10 cognitively normal (CN) controls, recruited via advertisements in a local newspaper. CN subjects were identified as individuals

who (i) were independently functioning community dwellers; (ii) did not have neurological or a personal or first degree relative history of psychiatric disorders; (iii) had no cognitive complaints; (iv) had a normal neurological and psychometric examination; (v) were not taking any psychoactive medications; (vi) had no history of head trauma; (vii) showed no signs of vascular pathology on MRI evaluation (Roman et al. 1993) and (ix) had a Mini-Mental State Examination (MMSE) (Folstein et al. 1975) score $\geq$ 29, a Neuropsychiatric Inventory (NPI) (Cummings et al. 1994) score of 0, and a Frontal Behavioral Inventory (FBI) (Kertesz et al. 1997) score of 0.

Demographic and clinical data for all subjects are shown in Table 1, with ratings of lobar atrophy (Kipps et al. 2007) and hypometabolism (Poljansky et al. 2011) for bvFTD patients shown in Table 2. All subjects and their caregivers provided written informed consent. The study protocol, approved by the Research Ethics Board of the Montreal Neurological Institute as well as by the Faculty of Medicine Research Ethics Office, McGill University, was carried out in accordance with the Declaration of Helsinki.

PET acquisition

3-(6-methyl-pyridin-2-ylethynyl)-cyclohex-2-enone-*O*-^{11}C-methyl-oxime ([^{11}C]ABP688) was synthesized as described previously (Elmenhorst et al. 2010) , with a radiochemical purity > 99%. The study was performed using a High-Resolution Research Tomograph (HRRT) PET scanner (CTI/Siemens, Knoxville, Tennessee), a brain dedicated tomograph combining high spatial image resolution with high sensitivity. Prior to radiopharmaceutical administration, a 6-minute transmission scan was acquired for scatter and attenuation correction using a [^{137}Cs] rotating point source. A 60-minute dynamic list-mode emission scan was started concomitantly with the venous injection of 370 MBq (mean specific activity >500 Ci/μmol) of [^{11}C]ABP688, with emission data acquired in list-mode format, and binned into 26 time frames. For each and every time frame, sets of fully 3D sinograms were generated from the list-mode data (2209 sinograms, span 9, with 256 radial bins and 288 azimuthal angle samples). A time-series of 26 3D images (frame duration: 6 × 30s, 4 × 60s, 8 × 120 s, 3 × 240 s, 5 × 300 s) were then reconstructed from

these sinograms, each 3D image being composed of 256 × 256 × 207 cubic voxels (voxel side-length of 1.21875 mm), using an expectation maximization image reconstruction algorithm with an ordinary Poisson model of the acquired PET data. The reconstruction included full accounting for the normalization, attenuation, and time-dependent scatter of random events. To reduce the partial volume effect, resolution modeling with point-spread function was implemented in the reconstruction (Comtat 2008). Subject head-motion correction was implemented using a data-driven motion estimation and correction method (Costes et al. 2009).

All patients underwent an [^{18}F]FDG PET scan using a Siemens ECAT EXACT HR + PET device (CTI/Siemens, Knoxville, TN, USA) as part of their clinical evaluation. In keeping with the ALARA radiation safety principle (Natarajan et al. 2013), data was not recollected on the HRRT. After fasting overnight, patients received a venous bolus injection of 185 MBq of ^{18}F-fluorodeoxyglucose ([^{18}F]FDG) in a quiet environment. A dynamic scan was performed in 3-dimenstional mode for 10 min under standard resting-state conditions with eyes open, recording 63 transaxial slices simultaneously with an axial resolution of 5 mm full width at half maximum (FWHM) and an in-plane resolution of 4.6 mm. Each collected slice had a thickness of 2.45 mm and a matrix size of 128 × 128 voxels. After correction for attenuation, scatter, decay and scanner-specific dead time, the PET data were reconstructed by filtered back-projection using a Hann filter (4.9 mm FWHM).

CN subjects had their acquisition conducted on the HRRT, with acquisition parameters identical to those for [^{11}C]ABP688, as described above. Images were reconstructed taking into consideration data acquired between 45-60 minutes only, with reconstruction matching that used for the HR+ data. In order to compare data from the HRRT and HR+ PET scanners, the resolution of the HRRT was matched to the partial volume effect of the HR+. To do so, an anisotropic Gaussian kernel of 5.7x5.7x6.7mm FWHM was used, which was found to be the best match of scanner resolutions through an internal phantom study (unpublished data). In the case of [^{18}F]FDG, two CN subjects were excluded owing to movement with one patient unable to return for the scan, reducing the sample size for [^{18}F]FDG to 4 bvFTD and 8 CN.

Magnetic Resonance Imaging

For anatomical co-registration and identification of the volumes of interest (VOI), all subjects underwent a high-resolution T-1 weighted MRI using a Siemens TRIO 3T scanner (Siemens Medical Solutions, Erlangen, Germany). Images were acquired in 3-D (voxel size=1mm^3; FOV=256x256 mm; TR=22 ms; TE=9.2 ms; Flip angle=30°), with the scan performed on either on the same day or less than 2 weeks apart from the PET acquisitions, depending on the availability of the research slots.

Imaging analysis

[^{11}C]ABP688 binding potential, non-displaceable (BP_{ND}) values were obtained using the simplified reference tissue method (SRTM) (Gunn et al. 1997), using the cerebellum as a reference region (Elmenhorst et al. 2009; Minuzzi et al. 2009). [^{18}F]FDG PET frames were summed and standardized uptake value ratio (SUV_R) maps calculated by normalizing the summed image to mean pontine activity for each subject. In order to correct for Partial volume error (PVE), a modified version (Greve et al. 2014; Rousset et al. 2007) of the Muller-Gartner method (Muller-Gartner et al. 1992; Rousset et al. 1998) was implemented using the PVElab software package (https://nru.dk/downloads/software/pveout/pveout.html) (Quarantelli et al. 2004).

Following correction for field inhomogeneities (Sled JG 1998), native MRI volumes were non-linearly resampled into standardized stereotaxic space, using the high-resolution ICBM template as reference (Fonov et al. 2009). Subsequently, normalized images were classified into grey matter (GM), white matter (WM) and cerebrospinal fluid (CSF) using an automatic algorithm (INSECT) (Zijdenbos A 1998). Voxel-based morphometry (VBM) (Ashburner and Friston, 2000) was carried out on the structural segmented GM images nonlinearly resampled to the standard stereotaxic space after blurring with an isotropic Gaussian kernel of 10mm FWHM. Finally, classified images were resampled to an anatomical template and automatically labeled using a probabilistic atlas based approach (ANIMAL) (Collins DL et al. 1999; Collins and Evans 1997). VOIs yielded by this procedure were subsequently applied to PET BP_{ND} (cerebellum) and SUV_R maps (pons).

Voxel-wise analysis maps of [^{11}C]ABP688 BP_{ND}, [^{18}F]FDG SUV_R , and VBM values were estimated using a basis functions approach (Gunn et al. 1997), with PET images convolved using an isotropic Gaussian kernel of 6mm FWHM. Parametric maps created in native space were then normalized into MNI space in order to allow for group comparisons. The resulting t-maps, calculated using RMINC (Lerch 2006), show the areas with a significant difference in BP_{ND}, SUV_R, and relative concentration of GM between groups. Those areas were subsequently adjusted for a statistical cluster-wise threshold of $p < 0.05$, and corrected for multiple comparisons using random field theory (Worsley et al. 1998). [^{11}C]ABP688 BP_{ND} local maxima coordinates were used to extract [^{18}F]FDG SUV_R , and VBM values, in order to compare the magnitude of decline.

Brain regions where all patients differed significantly from controls on the basis of Z scores ≥ 2—calculated using the formula [(individual patient value) - (control mean)/ (control standard deviation)]—were calculated for [^{11}C]ABP688 BP_{ND}, [^{18}F]FDG SUV_R , and VBM t-maps. These areas were then used to extract raw [^{11}C]ABP688 BP_{ND}, [^{18}F]FDG SUV_R , and VBM values, which, after reconversion to Z scores, were plotted using GraphPad Prism 5 software. Overlap maps—[^{11}C]ABP688 BP_{ND} and [^{18}F]FDG SUV_R, [^{11}C]ABP688 BP_{ND} and VBM, [^{18}F]FDG SUV_R and VBM—as well as areas showing only reduced [^{11}C]ABP688 BP_{ND}, [^{18}F]FDG SUV_R, and VBM—were created using MINC tools (http://www.bic.mni.mcgill.ca/ServicesSoftware/MINC). For overlap maps, binary masks were generated by applying the cluster-corrected t-map thresholds to each individual t-map—[^{11}C]ABP688 BP_{ND}, [^{18}F]FDG SUV_R, and VBM—setting voxels less than the given threshold to 0 and voxels greater than the threshold to 1. Binary masks were then summed, with voxels having a value of 2 indicating overlap. In order to show areas exhibiting only reductions (e.g. in availability of mGluR5) binary masks were subtracted (e.g. [^{11}C]ABP688 BP_{ND} - [^{18}F]FDG SUV_R - VBM), with the range of values in the resulting volume restricted to lie between 0 and 1, removing negative values generated as a result of the subtraction. Finally, volumes were visualized and color-coded using the software DISPLAY (http://www.bic.mni.mcgill.ca/software/Display/Display.html).

Results

Groups differed significantly in terms of MMSE, FBI and NPI (see Table 1). No differences were observed for age at scan, education, sex, or handedness. While all patients showed moderate hypometabolism within frontotemporal regions, atrophy ranged from very mild to moderate (see Table 2). Z score maps showing regions with significantly reduced [^{11}C]ABP688 BP_{ND}, hypometabolism and atrophy common to all patients—along with plots showing Z scores relative to controls (see Fig 1). Location and coordinates of local maxima for the contrast [^{11}C]ABP688 BP_{ND} CN > bvFTD] are reported in Table 3, along with values for [^{18}F]FDG SUV_R and VBM using these local maxima. Despite neurodegeneration being more widespread than declines in mGluR5 availability, hypometabolism and atrophy were found to be inferior to reductions in [^{11}C]ABP688 BP_{ND} in a wide range of FTLD predilection sites (see Table 3). Relative to controls, bvFTD patients showed reductions of 65 percent, 30 percent, and 15 percent—for [^{11}C]ABP688 BP_{ND}, [^{18}F]FDG SUV_R, and VBM, respectively—on the basis of values extracted from common Z score maps.

Voxel-wise analysis of group differences in [^{11}C]ABP688 BP_{ND} revealed declines in mGluR5 availability (85 152 mm^3) in orbital, ventromedial, and dorsomedial prefrontal areas (corrected for multiple comparisons, $p < 0.05$, df=13) (see Fig 2). Declines were likewise noted in the gyrus rectus, anterior cingulate (L>R), right posterior cingulate, superior frontal gyrus (L>R), paracentral lobule (L>R), caudate (L>R), left putamen, insula (R>L), thalamus (L>R), right lingual gyrus, and right cuneus. Additional declines were found in the right dorsolateral, right ventrolateral, and anterior prefrontal cortex, the right superior and middle temporal gyri, as well as in the temporal poles. No significant increases of [^{11}C]ABP688 binding were observed in bvFTD subjects.

Significant hypometabolism was noted among bvFTD patients (116 742 mm^3) in extensive prefrontal areas, including the orbitofrontal (R>L), ventromedial and dorsomedial prefrontal (L>R), and the cingulate gyrus (L>R) (corrected for multiple comparisons, $p < 0.05$) (see Fig 3). Metabolism was significantly reduced in the superior, middle, and inferior frontal gyri as well as in the precuneus and paracentral lobule (L>R). Hypometabolism was also found in the bilateral insula (R>L), uncus/amygdala,

and parahippocampus (L>R), as well as in subcortical structures, including the head of the caudatum and the left thalamus. There was also hypometabolism in the superior, middle, and inferior temporal gyri, temporal poles, and cerebellar tonsils.

Among bvFTD subjects, grey matter loss (88 845 mm^3) was predominantly focused in the striatum—including the putamen (L>R) and head of the caudate nucleus bilaterally (corrected for multiple comparisons, $p < 0.05$) (see Fig 4). There was significant involvement of the thalamus and insula bilaterally, as well as the amygdala, and parahippocampus. Atrophy was also observed in the anterior cingulate (L>R), precuneus (R>L) gyrus rectus, orbitofrontal gyrus, as well as the right superior/middle temporal gyri, though to a lesser degree (see table 3).

Overlap between [^{11}C]ABP688 BP_{ND} and [^{18}F]FDG SUV_R t-maps was observed in the gyrus rectus (L>R), anterior cingulate/ventromedial prefrontal cortex (L>R), dorsomedial prefrontal cortex (L>R), thalamus (L>R) insula (R>L) and temporal poles (22 379 mm^3; see Fig 5). [^{11}C]ABP688 BP_{ND} and VBM findings overlapped in the anterior cingulate/ventromedial prefrontal cortex (L>R), orbitofrontal cortex (R>L), thalamus (L>R), head of the caudate nucleus (L>R) and the insula (R>L) (13 463 mm^3; see Fig 6). Overlap between hypometabolic regions and atrophy was noted in medial and lateral orbitofrontal areas, anterior cingulate/ventromedial prefrontal cortex (L>R), dorsomedial prefrontal cortex (R>L), insula (R>L), thalamus (L>R), left amygdala, right hippocampal formation, and the head of the caudate nucleus (R>L) (14 179 mm^3; see Fig 7). Though hypometabolism and atrophy were found in frontal, temporal, and subcortical brain regions, these declines were found to be inferior relative to those for [^{11}C]ABP688 BP_{ND} in a wide range of areas, including the gyrus rectus, medial and lateral orbitofrontal cortex, ventromedial prefrontal cortex, left dorsomedial prefrontal cortex, paracentral lobule, frontal pole, left putamen, left insula, lingual gyrus, cuneus, temporal poles, right superior temporal gyrus, inferior and middle temporal gyri, and the right dorso- and ventrolateral prefrontal cortex.

Subtraction of binarized t-maps ([^{11}C]ABP688 BP_{ND} – [^{18}F]FDG SUV_R – VBM) showed that decreased binding of [^{11}C]ABP688 was unique to the gyrus rectus (R>L), orbitofrontal cortex (R>L), lateral portion of the right head of the caudate nucleus, left putamen, left superior temporal lobe, inferior

temporal lobes, temporal poles (R>L), right posterior cingulate, right ventral/dorsolateral prefrontal cortex, left paracentral lobule, right occipital cortex, and right lingual gyrus (55 742 mm^3; see Fig 8). A similar subtraction yielded a volume of 86 616 mm^3 for regions displaying only hypometabolism ([^{18}F]FDG SUV_R – [^{11}C]ABP688 BP_{ND} – VBM)—including the uncus/amygdalae (L>R), the parahippocampus (L>R), bilateral cuneus, posterior cingulate/precuneus (L>R), bilateral insula, medial prefrontal cortex, left posterior paracentral lobule, left frontal operculum, anterior temporal poles, orbitofrontal gyrus/gyrus rectus (R>L), and bilateral cerebellar cortex (see Fig 9). In addition, the orbitofrontal gyrus, the right middle temporal gyrus, right temporal operculum, left anterior insula, posterior insula bilaterally (R>L), ventral amygdala (L>R), left posterior inferior temporal gyrus, anterior cingulate gyrus (L>R), the putamen (L>R) and head of the caudate nucleus bilaterally, the thalamus as well as the posterior portion of the hippocampal formation, bilaterally, were found to be characterized only by GM reductions (VBM – [^{18}F]FDG SUV_R – [^{11}C]ABP688 BP_{ND}; 67 635 mm^3; see Fig 10). Though changes in [^{11}C]ABP688 BP_{ND}, [^{18}F]FDG SUVR, and VBM were found to co-exist within the orbitofrontal cortex and temporale lobe, relative to [^{18}F]FDG and VBM, findings for [^{11}C]ABP688 were more ventral and lateral, respectively.

Discussion

The present findings represent the first *in vivo* report of decreased availability of mGluR5 in bvFTD. In line with recent studies showing reduced binding of [^{11}C]ABP688 in disorders characterized by glutamate excitotoxicity—such as major depressive disorder and temporal lobe epilepsy (Choi et al. 2014; Deschwanden et al. 2011)—our findings may indicate increased glutamate levels in bvFTD. Further, we reproduced previous [^{18}F]FDG and VBM findings in terms of both the topography of neurodegeneration and its partially asymmetric distribution (Diehl-Schmid et al. 2007; Hornberger et al. 2012; Jeong et al. 2005; Pan et al. 2012). In addition, we showed that the volume of decreased mGluR5 availability was inferior to that for hypometabolism and GM atrophy, and that the overlap between reduced [^{11}C]ABP688 BP_{ND} and hypometabolism was superior to that for GM atrophy. Moreover, we showed that declines in

mGluR5 availability were unique to several isocortical, limbic, and paralimbic areas, possibly representing an early sign of pyramidal cell dysfunction. In this respect, the focality of [^{11}C]ABP688 BP_{ND} reductions in the present study is striking given the widespread distribution of mGluR5. In addition, several frontotemporal areas showed hypometabolism and/or GM loss in the absence of reduced [^{11}C]ABP688 binding. Taken together, these findings suggest a differential neuronal vulnerability to FTLD pathology in bvFTD—similar to that seen in other neurodegenerative diseases (Double et al. 2010)—with reduced availability of mGluR5 possibly preceding neurodegeneration within select frontotemporal brain regions.

While at physiological concentrations glutamate is known to play a pivotal role in synaptic plasticity (Balschun et al. 2006; Huber et al. 2001)—with any given function of a given cortical region likely to depend on glutamatergic neurotransmission at some level (Francis 2009)—at high concentrations it has been shown to act as a neurotoxin, promoting neuronal injury and death in animal models (Rao et al. 2001; Rothstein 1996) and in neurodegenerative diseases, including AD (Francis 2003). In the case of AD, accumulation of β-amyloid is thought to inhibit astroglial glutamate uptake, resulting in increased extracellular levels of glutamate, which, under chronic conditions, lead to cell death via sustained elevations in intracellular calcium (Harkany et al. 2000). This excitotoxic scenario may explain decreased binding of [^{11}C]ABP688 in that continued high levels of glutamate may alter the availability of its transmembrane allosteric binding site (Ametamey et al. 2007) by altering mGluR5 conformational states (Cabello et al. 2009; Canela et al. 2009; Changeux and Edelstein 2005; Romano et al. 1996). Indeed, affinity shifts in receptor-radioligand interactions have previously been described in the context of dopaminergic neurotransmission, where the affinity of a D2 PET radiopharmaceutical was altered following an amphetamine challenge (Narendran et al. 2004; Seneca et al. 2006; Wilson et al. 2005).

Recently, an expanded hexanucleotide repeat in the chromosome 9 open reading frame 72 (C9ORF72) was identified as the most common cause of familial FTD and amyotrophic lateral sclerosis (ALS), with mutations associated with deposition of TDP-43 pathology (DeJesus-Hernandez et al. 2011;

Renton et al. 2011). While the pathogenic mechanism(s) by which this repeat expansion could cause disease remain unknown, induced pluripotent stem cell differentiated neurons from C9ORF72 ALS patients were shown to be highly susceptible to glutamate excitotoxicity (Donnelly et al. 2013). Related work on primary cells from TDP-43 transgenic mice showed an increase vulnerability to the toxic effects of excess glutamate (Swarup et al. 2011). Moreover, a recent study involving transgenic mice expressing the FTDP-17 mutation P301L in the human tau gene—resulting in the accumulation of hyperphosphorylated tau—showed a tau dependent impairment of glutamate metabolism (Nilsen et al. 2013). These studies suggest that the pathogenicity of hyperphosphorylated tau and TDP-43—the molecular pathologies accounting for most cases of bvFTD (Mackenzie et al. 2011)—may involve glutamatergic excitotoxicity.

Certain methodological aspects, however, limit interpretation of the present findings. In addition to this study's cross sectional design and small sample size, the absence of histopathological data precludes conclusions about the homogeneity of the sample from the perspective of underlying molecular pathology. As such we were not able to address the possible interplay between different FTLD subtypes and possibly differing effects on mGluR5 availability. Moreover, potential limitations may accompany the use of VBM when applied to atrophic brains (Good et al. 2002).

Despite these caveats, our findings shed light on the possible role of glutamate excitotoxicity in the pathogenesis of bvFTD and suggest that [^{11}C]ABP688 may prove a suitable non-invasive marker of glutamatergic neurotransmission *in vivo*. Larger prospective studies are required to validate these findings, to establish the trajectory of reduced mGluR5 availability relative to other biomarkers of neurodegeneration, and to address the potential link between the dysregulation of glutamatergic neurotransmission and bvFTD symptomatology.

Acknowledgements

The authors wish to thank the patients and their families for participating in this study. This work was supported by the Canadian Institutes of Health Research (CIHR) [MOP-11-51-31], the Alan Tiffin Foundation, the Alzheimer's Association [NIRG-08-92090], and the Fonds de la recherche en santé du Québec (Chercheur boursier). The authors acknowledge the help of imaging staff at the Montreal Neurological Institute McConnell Brain Imaging Centre, including Reda Bouhachi, Simion Matei, and Rick Fukasawa (PET Technologists), Ron Lopez, David Costa, and Louise Marcott (MRI Technologists), and André Cormier (Chief MRI Technologist).

Conflict of Interest

The authors declare no conflict of interest.

References

Alladi S, Xuereb J, Bak T, Nestor P, Knibb J, Patterson K, Hodges JR (2007) Focal cortical presentations of Alzheimer's disease. Brain : a journal of neurology 130:2636-2645 doi:10.1093/brain/awm213

Ametamey SM, Treyer V, Streffer J, Wyss MT, Schmidt M, Blagoev M, Hintermann S, Auberson Y, Gasparini F, Fischer UC, Buck A (2007) Human PET studies of metabotropic glutamate receptor subtype 5 with 11C-ABP688. J Nucl Med 48:247-252

Ametamey SM, Kessler LJ, Honer M, Wyss MT, Buck A, Hintermann S, Auberson YP, Gasparini F, Schubiger PA (2006) Radiosynthesis and preclinical evaluation of 11C-ABP688 as a probe for imaging the metabotropic glutamate receptor subtype 5. J Nucl Med 47:698-705

Balschun D, Zuschratter W, Wetzel W (2006) Allosteric enhancement of metabotropic glutamate receptor 5 function promotes spatial memory. Neuroscience 142:691-702 doi:10.1016/j.neuroscience.2006.06.043

Cabello N, Gandía J, Bertarelli DC, Watanabe M, Lluís C, Franco R, Ferré S, Luján R, Ciruela F (2009) Metabotropic glutamate type 5, dopamine D2 and adenosine A2a receptors form higher-order oligomers in living cells. J Neurochem 109:1497-1507 doi:10.1111/j.1471-4159.2009.06078.x

Canela L, Fernández-Dueñas V, Albergaria C, Watanabe M, Lluís C, Mallol J, Canela EI, Franco R, Luján R, Ciruela F (2009) The association of metabotropic glutamate receptor type 5 with the neuronal Ca2+-binding protein 2 modulates receptor function. J Neurochem 111:555-567 doi:10.1111/j.1471-4159.2009.06348.x

Changeux J-P, Edelstein SJ (2005) Allosteric mechanisms of signal transduction. Science 308:1424-1428 doi:10.1126/science.1108595

Choi H, Kim YK, Oh SW, Im HJ, Hwang do W, Kang H, Lee B, Lee YS, Jeong JM, Kim EE, Chung JK, Lee DS (2014) In vivo imaging of mGluR5 changes during epileptogenesis using [11C]ABP688 PET in pilocarpine-induced epilepsy rat model. PloS One 9:e92765 doi:10.1371/journal.pone.0092765

Collins DL, Zijendos AP, Barré WFC, Evans AC (1999) ANIMAL+INSECT: inproved cortical structure segmentation (1999). In: Kuba A, Samal M, Todd-Pokropek A (eds) Lecture Notes in Computer Science, Springer-Verlag Berlin Heidelberg, pp 210–223

Collins L, Evans A (1997) Animal: validation and applications of non-linear registration-based segmentation. Int J Pattern Recogn Art Intell 1271–1294

Comtat C, Sureau FC, Sibomana M, Hong IK, Sjoholm N, Trebossen R. Image based resolution modeling for the HRRT OSEM reconstructions software (2008). In: IEEE Nuclear Science Symposium Conference Record, pp 4120-4123

Costes N, Dagher A, Larcher K, Evans AC, Collins DL, Reilhac A (2009) Motion correction of multi-frame PET data in neuroreceptor mapping: simulation based validation. NeuroImage 47:1496-1505. doi:10.1016/j.neuroimage.2009.05.052

Cummings JL, Mega M, Gray K, Rosenberg-Thompson S, Carusi DA, Gornbein J (1994) The Neuropsychiatric Inventory: comprehensive assessment of psychopathology in dementia Neurology 44:2308-2314

Dalfo E, Albasanz JL, Rodriguez A, Martin M, Ferrer I (2005) Abnormal group I metabotropic glutamate receptor expression and signaling in the frontal cortex in Pick disease. J Neuropathol Exp Neurol 64:638-647

DeJesus-Hernandez M, Mackenzie IR, Boeve BF, Boxer AL, Baker M, Rutherford NJ, Nicholson AM, Finch NA, Flynn H, Adamson J, Kouri N, Wojtas A, Sengdy P, Hsiung GY, Karydas A, Seeley WW, Josephs KA, Coppola G, Geschwind DH, Wszolek ZK, Feldman H, Knopman DS, Petersen RC, Miller BL, Dickson DW, Boylan KB, Graff-Radford NR, Rademakers R (2011) Expanded GGGGCC hexanucleotide repeat in noncoding region of C9ORF72 causes chromosome 9p-linked FTD and ALS. Neuron 72:245-256. doi:10.1016/j.neuron.2011.09.011

Deschwanden A, Karolewicz B, Feyissa AM, Treyer V, Ametamey SM, Johayem A, Burger C, Auberson YP, Sovago J, Stockmeier CA, Buck A, Hasler G (2011) Reduced metabotropic glutamate

receptor 5 density in major depression determined by [(11)C]ABP688 PET and postmortem study. Am J Psychiatry 168:727-734. doi:10.1176/appi.ajp.2011.09111607

Diehl-Schmid J, Grimmer T, Drzezga A, Bornschein S, Riemenschneider M, Förstl H, Schwaiger M, Kurz A (2007) Decline of cerebral glucose metabolism in frontotemporal dementia: a longitudinal 18F-FDG-PET-study. Neurobiol Aging 28:42-50. doi:10.1016/j.neurobiolaging.2005.11.002

Donnelly CJ, Zhang PW, Pham JT, Haeusler AR, Mistry NA, Vidensky S, Daley EL, Poth EM, Hoover B, Fines DM, Maragakis N, Tienari PJ, Petrucelli L, Traynor BJ, Wang J, Rigo F, Bennett CF, Blackshaw S, Sattler R, Rothstein JD (2013) RNA toxicity from the ALS/FTD C9ORF72 expansion is mitigated by antisense intervention. Neuron 80:415-428. doi:10.1016/j.neuron.2013.10.015

Double KL, Reyes S, Werry EL, Halliday GM (2010) Selective cell death in neurodegeneration: why are some neurons spared in vulnerable regions? Prog Neurobiol 92:316-329. doi:10.1016/j.pneurobio.2010.06.001

Elmenhorst D, Biagini M, Minuzzi L, Aliaga A, Massarweh G, Diksic M, Avoli M, Bauer A,Rosa-Neto P (2009) Evaluation of reference models for [11C]ABP688 targeting the metabotropic glutamate receptor 5 in rats-application to an epilepsy model. J Cerebr Blood F Met 29:S71-S72

Elmenhorst D, Minuzzi L, Aliaga A, Rowley J, Massarweh G, Diksic M, Bauer A, Rosa-Neto P (2010) In vivo and in vitro validation of reference tissue models for the mGluR(5) ligand [(11)C]ABP688. J Cereb Blood Flow Metab 30:1538-1549. doi:10.1038/jcbfm.2010.65

Ferraguti F, Shigemoto R (2006) Metabotropic glutamate receptors. Cell Tissue Res 326:483-504. doi:10.1007/s00441-006-0266-5

Ferrer I (1999) Neurons and their dendrites in frontotemporal dementia. Dement Geriatr Cogn Disord 10 Suppl 1:55-60. doi:51214

Folstein MF, Folstein SE, McHugh PR (1975) "Mini-mental state". A practical method for grading the cognitive state of patients for the clinician. J Psychiatr Res12:189-198

Francis PT (2009) Altered glutamate neurotransmission and behaviour in dementia: evidence from studies of memantine. Curr Mol Pharmacol 2:77-82

Francis PT (2003) Glutamatergic systems in Alzheimer's disease. Int J Geriatr Psychiatry 18:S15-21. doi:10.1002/gps.934

Goetz CG, Fahn S, Martinez-Martin P, Poewe W, Sampaio C, Stebbins GT, Stern MB, Tilley BC, Dodel R, Dubois B, Holloway R, Jankovic J, Kulisevsky J, Lang AE, Lees A, Leurgans S, LeWitt PA, Nyenhuis D, Olanow CW, Rascol O, Schrag A, Teresi JA, Van Hilten JJ, LaPelle N (2007) Movement Disorder Society-sponsored revision of the Unified Parkinson's Disease Rating Scale (MDS-UPDRS): Process, format, and clinimetric testing plan. Mov Disord 22:41-47. doi:10.1002/mds.21198

Good CD, Scahill RI, Fox NC, Ashburner J, Friston KJ, Chan D, Crum WR, Rossor MN, Frackowiak RS (2002) Automatic differentiation of anatomical patterns in the human brain: validation with studies of degenerative dementias. Neuroimage 17:29-46

Greve DN, Svarer C, Fisher PM, Feng L, Hansen AE, Baare W, Rosen B, Fischl B, Knudsen GM (2014) Cortical surface-based analysis reduces bias and variance in kinetic modeling of brain PET data. Neuroimage 92:225-236. doi:10.1016/j.neuroimage.2013.12.021

Gunn RN, Lammertsma AA, Hume SP, Cunningham VJ (1997) Parametric imaging of ligand-receptor binding in PET using a simplified reference region model. Neuroimage 6:279-287. doi:10.1006/nimg.1997.0303

Harkany T, Abrahám I, Timmerman W, Laskay G, Tóth B, Sasvári M, Kónya C, Sebens JB, Korf J, Nyakas C, Zarándi M, Soós K, Penke B, Luiten PG (2000) beta-amyloid neurotoxicity is mediated by a glutamate-triggered excitotoxic cascade in rat nucleus basalis. Eur J Neurosci 12:2735-2745

Hornberger M, Wong S, Tan R, Irish M, Piguet O, Kril J, Hodges JR, Halliday G (2012) In vivo and post-mortem memory circuit integrity in frontotemporal dementia and Alzheimer's disease. Brain 135:3015-3025. doi:10.1093/brain/aws239

Huber KM, Roder JC, Bear MF (2001) Chemical induction of mGluR5- and protein synthesis--dependent long-term depression in hippocampal area CA1. J Neurophysiol 86:321-325

Jeong Y, Cho SS, Park JM, Kang SJ, Lee JS, Kang E, Na DL, Kim SE (2005) 18F-FDG PET findings in frontotemporal dementia: an SPM analysis of 29 patients J Nucl Med46:233-239

Kertesz A, Davidson W, Fox H (1997) Frontal behavioral inventory: diagnostic criteria for frontal lobe dementia. Can J Neurol Sci 24:29-36

Kipps CM, Davies RR, Mitchell J, Kril JJ, Halliday GM, Hodges JR (2007) Clinical significance of lobar atrophy in frontotemporal dementia: application of an MRI visual rating scale Dementia and geriatric cognitive disorders 23:334-342 doi:10.1159/000100973

Lerch J (2006) Voxel-wise morphometry using RMINC. http://www.bic.mni.mcgill.ca/~samir/Brain_imaging/RMINC.pdf. Accessed July 15, 2014

Llansola M, Felipo V (2010) Metabotropic glutamate receptor 5, but not 1, modulates NMDA receptor-mediated activation of neuronal nitric oxide synthase. Neurochem Int 56:535-545. doi:10.1016/j.neuint.2009.12.016

Mackenzie IR, Munoz DG, Kusaka H, Yokota O, Ishihara K, Roeber S, Kretzschmar HA, Cairns NJ, Neumann M (2011) Distinct pathological subtypes of FTLD-FUS. Acta neuropathol 121:207-218. doi:10.1007/s00401-010-0764-0

Mackenzie IR, Neumann M, Bigio EH, Cairns NJ, Alafuzoff I, Kril J, Kovacs GG, Ghetti B, Halliday G, Holm IE, Ince PG, Kamphorst W, Revesz T, Rozemuller AJ, Kumar-Singh S, Akiyama H, Baborie A, Spina S, Dickson DW, Trojanowski JQ, Mann DM (2010) Nomenclature and nosology for neuropathologic subtypes of frontotemporal lobar degeneration: an update. Acta neuropathol 119:1-4. doi:10.1007/s00401-009-0612-2

Mendez MF, Lauterbach EC, Sampson SM; ANPA Committee on Research (2008) An evidence-based review of the psychopathology of frontotemporal dementia: a report of the ANPA Committee on Research. J Neuropsychiatry Clin Neurosci 20:130-149. doi:10.1176/appi.neuropsych.20.2.130

Minuzzi L, Diksic M, Gauthier S, Quirion R, Rosa-Neto P (2009) In vitro quantification of mGluR5 in pons and cerebellum of human brain using [H-3]ABP688. J Cerebr Blood F Met 29:S368-S369

Muller-Gartner HW, Links JM, Prince JL, Bryan RN, McVeigh E, Leal JP, Davatzikos C, Frost JJ (1992) Measurement of radiotracer concentration in brain gray matter using positron emission tomography: MRI-based correction for partial volume effects. J Cereb Blood Flow Metab 12:571-583. doi:10.1038/jcbfm.1992.81

Narendran R, Hwang DR, Slifstein M, Talbot PS, Erritzoe D, Huang Y (2004) In vivo vulnerability to competition by endogenous dopamine: comparison of the D2 receptor agonist radiotracer (-)-N-[11C]propyl-norapomorphine ([11C]NPA) with the D2 receptor antagonist radiotracer [11C]-racloprid. Synapse 52:188-208. doi:10.1002/syn.20013

Natarajan MK, Paul N, Mercuri M, Waller EJ, Leipsic J, Traboulsi M, Banijamali HS, Benson L, Sheth TN; Secondary Panel:, Simpson CS, Brydie A, Love MP, Gallo R; Canadian Cardiovascular Society (2013) Canadian Cardiovascular Society position statement on radiation exposure from cardiac imaging and interventional procedures. Can J Cardiol 29:1361-1368. doi:10.1016/j.cjca.2013.06.002

Nilsen LH, Rae C, Ittner LM, Gotz J, Sonnewald U (2013) Glutamate metabolism is impaired in transgenic mice with tau hyperphosphorylation. J Cereb Blood Flow Metab 33:684-691. doi:10.1038/jcbfm.2012.212

Niswender CM, Conn PJ (2010) Metabotropic glutamate receptors: physiology, pharmacology, and disease. Annu Rev Pharmacol Toxicol 50:295-322. doi:10.1146/annurev.pharmtox.011008.145533

Pan PL, Song W, Yang J, Huang R, Chen K, Gong QY, Zhong JG, Shi HC, Shang HF (2012) Gray matter atrophy in behavioral variant frontotemporal dementia: a meta-analysis of voxel-based morphometry studies. Dement Geriatr Cogn Disord. 33:141-148 doi:10.1159/000338176

Perroy J, Raynaud F, Homburger V, Rousset MC, Telley L, Bockaert J, Fagni L (2008) Direct interaction enables cross-talk between ionotropic and group I metabotropic glutamate receptors. J Biol Chem 283:6799-6805. doi:10.1074/jbc.M705661200

Poljansky S, Ibach B, Hirschberger B, Manner P, Klunemann H, Hajak G, Marienhagen J (2011) A visual [18F]FDG-PET rating scale for the differential diagnosis of frontotemporal lobar degeneration European archives of psychiatry and clinical neuroscience 261:433-446 doi:10.1007/s00406-010-0184-0

Procter AW, Qurne M, Francis PT (1999) Neurochemical features of frontotemporal dementia. Dement Geriatr Cogn Disord 10 Suppl 1:80-84. doi:51219

Quarantelli M et al. (2004) Integrated software for the analysis of brain PET/SPECT studies with partial-volume-effect correction. J Nucl Med 45:192-201

Rao VL, Bowen KK, Dempsey RJ (2001) Transient focal cerebral ischemia down-regulates glutamate transporters GLT-1 and EAAC1 expression in rat brain. Neurochem Res 26:497-502

Rascovsky K, Hodges JR, Knopman D, Mendez MF, Kramer JH, Neuhaus J, van Swieten JC, Seelaar H, Dopper EG, Onyike CU, Hillis AE, Josephs KA, Boeve BF, Kertesz A, Seeley WW, Rankin KP, Johnson JK, Gorno-Tempini ML, Rosen H, Prioleau-Latham CE, Lee A, Kipps CM, Lillo P, Piguet O, Rohrer JD, Rossor MN, Warren JD, Fox NC, Galasko D, Salmon DP, Black SE, Mesulam M, Weintraub S, Dickerson BC, Diehl-Schmid J, Pasquier F, Deramecourt V, Lebert F, Pijnenburg Y, Chow TW, Manes F, Grafman J, Cappa SF, Freedman M, Grossman M, Miller BL. (2011) Sensitivity of revised diagnostic criteria for the behavioural variant of frontotemporal dementia. Brain 134:2456-2477. doi:10.1093/brain/awr179

Ratnavalli E, Brayne C, Dawson K, Hodges JR (2002) The prevalence of frontotemporal dementia Neurology 58:1615-1621

Renton AE, Majounie E, Waite A, Simón-Sánchez J, Rollinson S, Gibbs JR, Schymick JC, Laaksovirta H, van Swieten JC, Myllykangas L, Kalimo H, Paetau A, Abramzon Y, Remes AM, Kaganovich A, Scholz SW, Duckworth J, Ding J, Harmer DW, Hernandez DG, Johnson JO, Mok K, Ryten M, Trabzuni D, Guerreiro RJ, Orrell RW, Neal J, Murray A, Pearson J, Jansen IE, Sondervan D, Seelaar H, Blake D, Young K, Halliwell N, Callister JB, Toulson G, Richardson A, Gerhard A, Snowden J, Mann D, Neary D, Nalls MA, Peuralinna T, Jansson L, Isoviita VM, Kaivorinne AL, Hölttä-Vuori M, Ikonen E, Sulkava R, Benatar M, Wuu J, Chiò A, Restagno G, Borghero G, Sabatelli M; ITALSGEN Consortium, Heckerman D, Rogaeva E, Zinman L, Rothstein JD, Sendtner M, Drepper C, Eichler EE, Alkan C, Abdullaev Z, Pack SD, Dutra A, Pak E, Hardy J, Singleton A, Williams NM, Heutink P, Pickering-Brown S, Morris HR, Tienari PJ, Traynor BJ (2011) A hexanucleotide repeat expansion in C9ORF72 is the cause of chromosome 9p21-linked ALS-FTD. Neuron 72:257-268. doi:10.1016/j.neuron.2011.09.010

Roman GC, Tatemichi TK, Erkinjuntti T, Cummings JL, Masdeu JC, Garcia JH, Amaducci L, Orgogozo JM, Brun A, Hofman A, Moody DM, O'Brien MD, Yamaguchi T, Grafman J, Drayer BP, Bennett DA, Fisher M, Ogata J, Kokmen E, Bermejo F, Wolf PA, Gorelick PB, Bick KL, Pajeau AK, Bell MA, DeCarli C, Culebras A, Korczyn AD, Bogousslavsky J, Hartmann A, Scheinberg P (1993) Vascular dementia: diagnostic criteria for research studies. Report of the NINDS-AIREN International Workshop. Neurology 43:250-260

Romano C, Yang WL, O'Malley KL (1996) Metabotropic glutamate receptor 5 is a disulfide-linked dimer. J Biol Chem 271:28612-28616

Rosso SM, Donker Kaat L, Baks T, Joosse M, de Koning I, Pijnenburg Y, de Jong D, Dooijes D, Kamphorst W, Ravid R, Niermeijer MF, Verheij F, Kremer HP, Scheltens P, van Duijn CM, Heutink P, van Swieten JC (2003) Frontotemporal dementia in The Netherlands: patient characteristics and prevalence estimates from a population-based study. Brain 126:2016-2022. doi:10.1093/brain/awg204

Rothstein JD (1996) Excitotoxicity hypothesis. Neurology 47:S19-26

Rousset O, Rahmim A, Alavi A, Zaidi H (2007) Partial Volume Correction Strategies in PET. PET Clinics 2:235-249

Rousset OG, Ma Y, Evans AC (1998) Correction for partial volume effects in PET: principle and validation. J Nucl Med 39:904-911

Schaeffer E, Duplantier A (2010) Glutamate and Neurodegenerative Disease. In: Dominguez C (ed) Neurodegnerative Diseases. Springer-Verlag Berlin Heidelberg, Heidelberg, pp 91-147

Seneca N, Finnema SJ, Farde L, Gulyas B, Wikstrom HV, Halldin C, Innis RB (2006) Effect of amphetamine on dopamine D2 receptor binding in nonhuman primate brain: a comparison of the agonist radioligand [11C]MNPA and antagonist [11C]raclopride. Synapse 59:260-269. doi:10.1002/syn.20238

Sled JG ZA, Evans AC. A (1998) A nonparametric method for automatic correction of intensity nonuniformity in MRI data. IEEE Trans Med Imag 17:87–97

Swartz JR, Miller BL, Lesser IM, Booth R, Darby A, Wohl M, Benson DF (1997) Behavioral phenomenology in Alzheimer's disease, frontotemporal dementia, and late-life depression: a retrospective analysis. J Geriatr Psychiatry Neurol 10:67-74

Swarup V, Phaneuf D, Dupre N, Petri S, Strong M, Kriz J, Julien JP (2011) Deregulation of TDP-43 in amyotrophic lateral sclerosis triggers nuclear factor kappaB-mediated pathogenic pathways. J Exp Med 208:2429-2447. doi:10.1084/jem.20111313

Wilson AA, McCormick P, Kapur S, Willeit M, Garcia A, Hussey D, Houle S, Seeman P, Ginovart N (2005) Radiosynthesis and evaluation of [11C]-(+)-4-propyl-3,4,4a,5,6,10b-hexahydro-2H-naphtho[1,2-b][1,4]oxazin-9-ol as a potential radiotracer for in vivo imaging of the dopamine D2 high-affinity state with positron emission tomography. J Med Chem 48:4153-4160. doi:10.1021/jm050155n

Worsley KJ, Cao J, Paus T, Petrides M, Evans AC (1998) Applications of random field theory to functional connectivity. Hum Brain Mapp 6:364-367

Zijdenbos A FR, Evans A (1998) Automatic quantification of MS lesions in 3D MRI brain data sets: validation of INSECT. In: Wells M, Colchester A, Delp S (eds). Lecture Notes in Computer Science. Springer, Berlin Heidelberg New York, pp. 438-448

Tables and Figures

Table 1 Demographic and clinical data for all subjects.

	BvFTD (n=5)	***CN (n=10)***	***P*[a] value**
Age at scan, Med (IQR), years	65 (7)	63 (2.75)	0.65
Education, Med (IQR), years	10 (5)	16 (4)	0.06
Sex, M/F	3/2	7/3	1.00
Handedness, R/L	5/0	9/1	0.52
MMSE, Med (IQR), max=30	26 (1)	30 (1)	0.03
FBI, Med (IQR), max= 72	20 (0)	0 (0)	0.001
NPI Total, Med (IQR), max= 144	32 (8)	0 (0)	0.001

Due to the small group sizes, data are represented as Med (IQR)= median (interquartile range).

Abbreviations: M/F= Male/Female; R/L= Right/Left; MMSE= Mini-mental state examination; FBI= Frontal Behavioral Inventory; NPI= Neuropsychiatric Inventory.

[a] The t test for continuous variables, Fischer's exact test for categorical variables.

Table 2 Ratings of hypometabolism and lobar atrophy in patients with bvFTD.

	[^{18}F]FDG-PET							MRI	
Subject	**Frontal Lobe**	**Temporal Lobe**	**Parietal Lobe**	**Occipital Lobe**	**Cerebellum**	**Basal Ganglia**	**Thalamus**	**Frontal Lobe**	**Anterior Temporal Lobe**
1	2	2	1	0	0	0	1	3	2
2	2	2	1	0	0	0	0	1	1
3	2	2	1	0	0	0	0	3	3
4	2	2	1	0	0	0	0	1	2
5	2	2	1	0	0	0	1	1	2

Ratings for [^{18}F]FDG-PET: 0=absent, 1=mild, 2=moderate, 3=strong.

Ratings for MRI: 1=very mild, 2=mild, 3=moderate.

Table 3 Location and Talairach coordinates of local maxima for areas of reduced [^{11}C]ABP688 BP_{ND} in patients with bvFTD, along with t-values for [^{18}F]FDG SUV_R and VBM findings, using [^{11}C]ABP688 BP_{ND} maxima coordinates.

Brain region	**x**	**y**	**z**	$t_{[11C]ABP688}$	**P**	$t_{[18F]FDG}$	**P**	t_{VBM}	**P**
Gyrus rectus L	-9.0	28.2	-24.7	-7.12	>0.0001	-4.19	>0.0001	-2.28	0.0401
Gyrus rectus R	13.8	26.2	-24.7	-6.52	>0.0001	-3.22	0.0092	-2.38	0.0333
Medial orbitofrontal cortex L	-16.0	23.1	-15.2	-8.49	>0.0001	-2.40	0.0373	-0.527	0.6071
Medial orbitofrontal cortex R	15.0	-15.2	-9.66	-9.73	>0.0001	-1.98	0.0076	-0.002	0.9998
Lateral orbitofrontal cortex L	-32.1	36.0	-15.2	-4.63	0.0005	-4.14	0.0020	-4.03	0.0014
Lateral orbitofrontal cortex R	28.1	47.2	-15.2	-5.21	0.0002	2.59	0.0269	-4.45	0.0007
Ventromedial prefrontal cortex L	-2.9	51.3	4.0	-7.42	>0.0001	-5.55	0.0002	-5.6t9	>0.0001
Ventromedial prefrontal cortex R	13.3	53.2	2.5	-4.42	0.0007	-2.01	0.0722	-3.32	0.0055
Dorsomedial prefrontal cortex L	-3.6	56.9	28.0	-6.14	>0.0001	-4.56	0.0010	-1.43	0.1763
Dorsomedial prefrontal cortex R	3.3	42.0	34.2	-4.11	0.0012	-4.88	0.0006	-4.29	0.0009
Anterior cingulate L	-2.4	37.0	14.7	-4.93	0.0003	-4.03	0.0024	-5.00	0.0002
Anterior cingulate R	5.0	40.2	14.7	-4.40	0.0007	-3.97	0.0026	-5.66	>0.0001
Frontal pole L	-10.1	71.1	3.0	-4.85	0.0003	-2.79	0.0191	-1.53	0.1500
Frontal pole R	14.2	72.0	3.0	-4.81	0.0003	-2.59	0.0269	-1.42	0.1791
Dorsolateral prefrontal cortex L	--	--	--	--	--	--	--	--	--
Dorsolateral prefrontal cortex R	52.1	25.1	21.8	-8.3	>0.0001	-5.01	0.0005	-1.51	0.1550
Ventrolateral prefrontal cortex L	--	--	--	--	--	--	--	--	--
Ventrolateral prefrontal cortex R	52.1	38.9	-4.9	-5.87	>0.0001	-5.28	0.0004	-0.96	0.3546
Paracentral lobule L	-4.6	-26.9	64.5	-5.09	0.0002	-1.98	0.0759	-2.34	0.0359
Paracentral lobule R	7.0	-35.9	-55.1	-4.11	0.0002	-1.98	0.0759	-1.52	0.0152

Thalamus L	-17.8	-31.3	1.8	-6.50	>0.0001	-3.11	0.0111	-8.74	>0.0001
Thalamus R	9.0	-15.9	1.8	-4.74	0.0004	-1.93	0.0824	-9.66	>0.0001
Hypothalamus L	-5.1	-5.9	-11.1	-4.18	0.0011	-2.32	0.0428	-8.49	>0.0001
Hypothalamus R	4.1	-5.9	-11.2	-4.26	0.0009	-2.67	0.0235	-8.34	>0.0001
Caudate L	-11.2	14.1	1.8	-5.43	0.0001	-4.65	0.0009	-5.89	>0.0001
Caudate R	9.0	9.1	7.3	-3.96	0.0016	-4.16	0.0019	-1.05	0.3128
Putamen L	-26.2	17.1	1.8	-4.74	0.0004	-3.64	0.0445	-3.81	0.0022
Putamen R	--	--	--	--	--	--	--	--	--
Insula L	-41.1	13.0	-9.8	-4.55	0.0005	-3.59	0.0049	-4.11	0.0012
Insula R	41.7	14.1	-2.0	-5.76	>0.0001	-4.32	0.0015	-5.78	>0.0001
Temporal pole L	-38.1	22.2	-35.9	-5.59	>0.0001	-4.13	0.0020	-2.02	0.0645
Temporal pole R	31.1	22.2	-39.0	-6.79	>0.0001	-2.75	0.0205	-1.56	0.1428
Superior temporal gyrus L	-58.2	-10.9	2.0	-3.96	0.0016	-4.07	0.0023	-1.74	0.1055
Superior temporal gyrus R	49.4	-2.4	-4.0	-6.61	>0.0001	-3.21	0.0093	-4.78	0.0004
Middle temporal gyrus L	-58.2	-16.0	-11.0	-4.60	0.0005	-4.00	0.0024	-1.29	0.2195
Middle temporal gyrus R	52.7	-12.1	-24.0	-6.99	>0.0001	-4.53	0.0011	-1.53	0.1500
Inferior temporal gyrus L	-58.2	-24.5	-25.4	-7.19	>0.0001	-3.95	0.0027	-0.16	0.8753
Inferior temporal gyrus R	52.7	-45.1	-22.9	-5.16	0.0002	-3.65	0.0045	-0.09	0.9297
Hippocampal formation L	-35.1	-11.8	-19.2	-4.94	0.0003	-1.00	0.3409	-1.62	0.1292
Hippocampal formation R	34.5	-14.6	-18.5	-1.99	0.0680	-2.77	0.0198	-3.26	0.0062
Cuneus L	-11.2	-92.9	15.9	-5.22	0.0002	-3.35	0.0074	-4.81	0.0003
Cuneus R	13.8	-90.8	15.9	-5.27	0.0002	-2.05	0.0611	-4.69	0.0004
Lingual gyrus L	-12.7	-73.7	-1.7	-6.87	>0.0001	-1.27	0.2328	-5.52	>0.0001
Lingual gyrus R	22.8	-79.1	-3.9	-7.17	>0.0001	-0.41	0.6905	-0.26	0.7983

Abbreviations: standardized uptake ratio (SUV_R); voxel based morphometry (VBM); non-displaceable binding potentials (BP_{ND}). Talairach coordinates (x, y, z) of [^{11}C]ABP688 BP_{ND} local maxima (t-values, corrected for multiple comparisons, $p < 0.05$) were applied to [^{18}F]FDG SUV_R and VBM t-maps in order to extra t-values. P values were determined using t-values and degrees of freedom ([^{11}C]ABP688 BP_{ND}, =14, [^{18}F]FDG SUV_R = 13, VBM =14). R= Right hemisphere; L=Left hemisphere. -- Indicates no findings in that region.

Fig. 1 Z score maps for all bvFTD patients were created for [^{11}C]ABP688 BP_{ND}, [^{18}F]FDG SUV_R, and VBM. These maps were then combined to show areas with significantly reduced [^{11}C]ABP688 BP_{ND}, [^{18}F]FDG SUV_R, and GM common to all bvFTD patients (top left, top right, bottom left, respectively). These common Z maps were then used to extract raw [^{11}C]ABP688 BP_{ND}, [^{18}F]FDG SUV_R, and VBM values. After conversion to Z scores, values were plotted, relative to CN subjects (bottom right). *** $p < 0.001$ ** $p < 0.01$ * $p < 0.05$

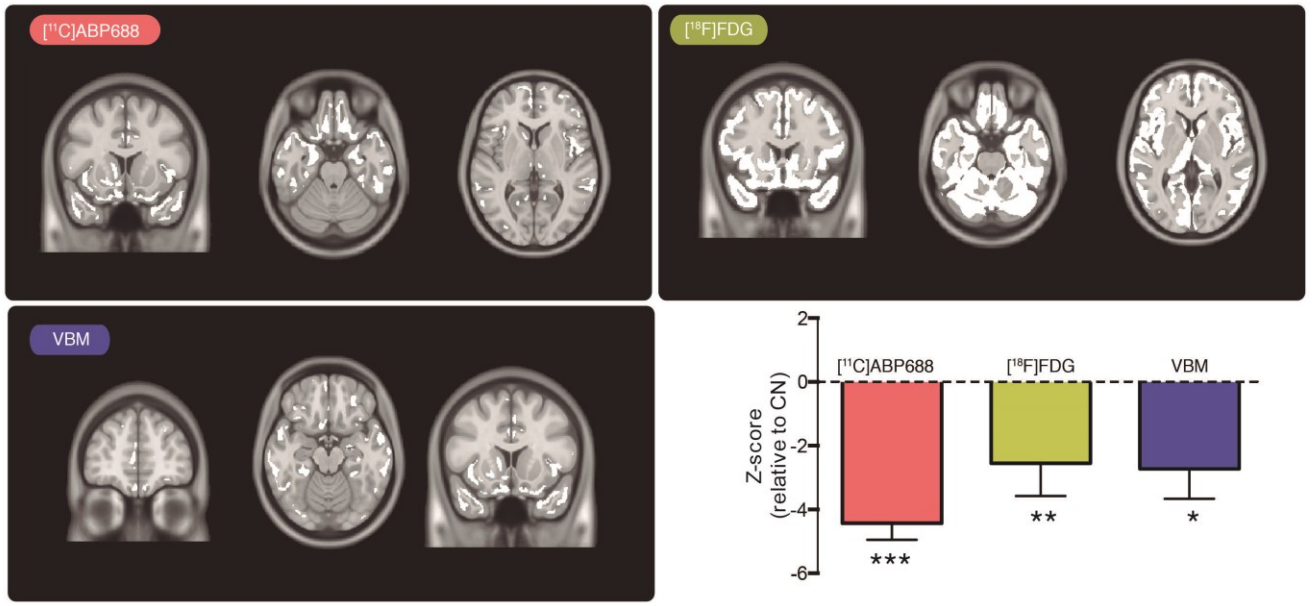

Fig. 2 Voxel-wise t-maps showing areas of decreased [^{11}C]ABP688 BP_{ND} in patients with bvFTD compared with CN subjects (85 152 mm^3; corrected for multiple comparisons, $p < 0.05$). Leftward asymmetry was noted in the anterior cingulate, superior frontal gyrus, paracentral lobule, caudate, putamen, and thalamus. Rightward asymmetry was found in the posterior cingulate, lingual gyrus, cuneus, dorsolateral/ventrolateral prefrontal cortex, superior/middle temporal gyri and the temporal poles. No significant increases of [^{11}C]ABP688 binding were observed in bvFTD subjects.

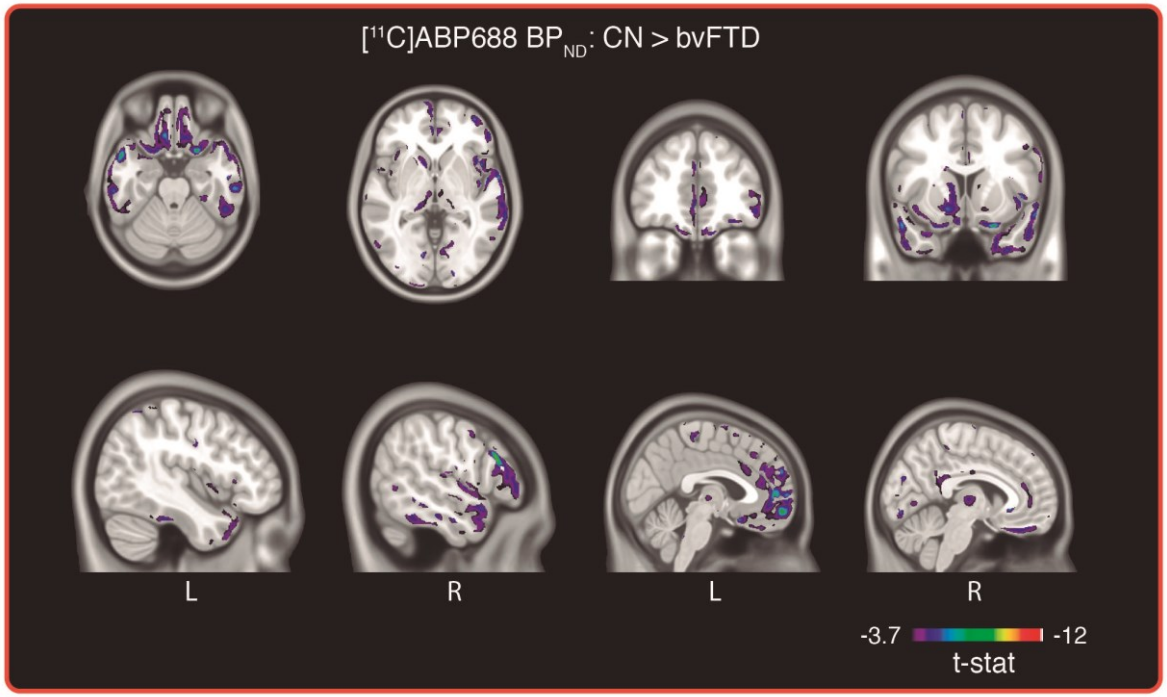

Fig. 3 Voxel-wise t-maps showing areas of decreased [^{18}F]FDG SUV_R in patients with bvFTD compared with CN subjects (116 742 mm^3; corrected for multiple comparisons, $p < 0.05$). The dorso/ventromedial prefrontal cortex, cingulate gyrus, frontal gyri, paracentral lobule, precuneus, parahippocampus, thalamus, caudate and temporal lobes were characterized by leftward asymmetry. Hypometabolism was also noted with rightward asymmetry in the insula and orbitofrontal gyrus and in the cerebellar tonsils bilaterally.

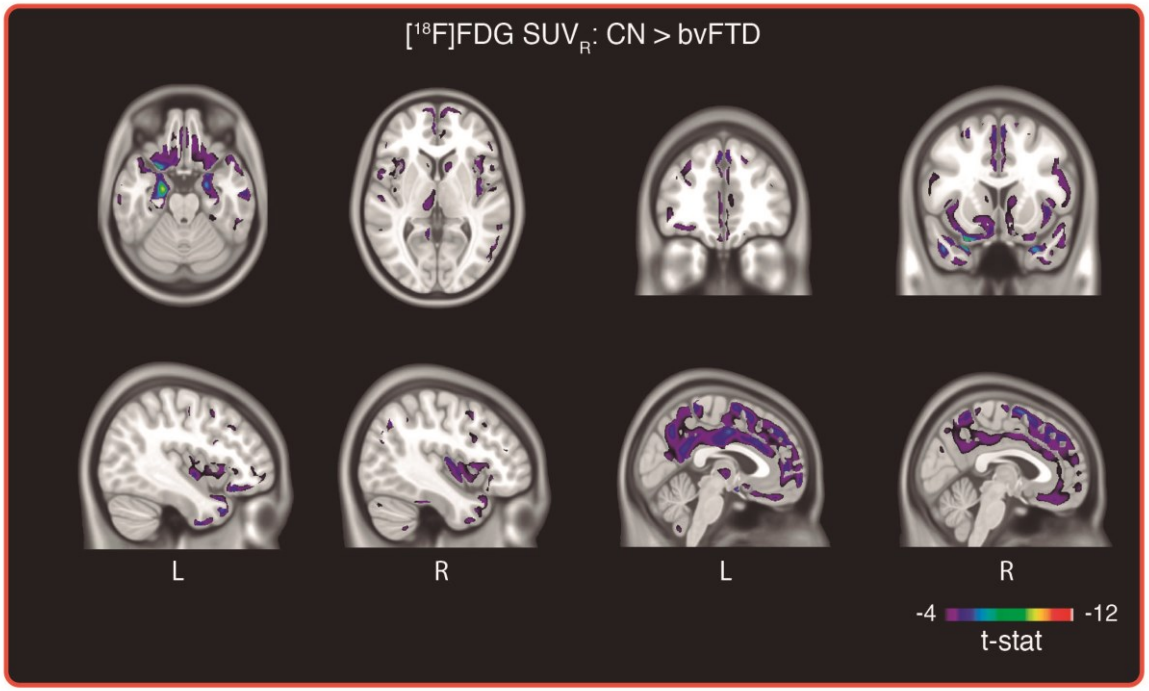

Fig. 4 Voxel-wise t-maps showing areas of reduced VBM derived GM concentration in patients with bvFTD compared with CN subjects (88 845 mm^3; corrected for multiple comparisons, $p < 0.05$). Atrophy was predominant in the thalami (L>R), head of caudate, insula, uncus/amygdala, and parahippocampus. GM loss was likewise noted in the putamen (L>R), precuneus (R>L), anterior cingulate (L>R), gyrus rectus, orbitofrontal gyrus and right superior/middle temporal gyri.

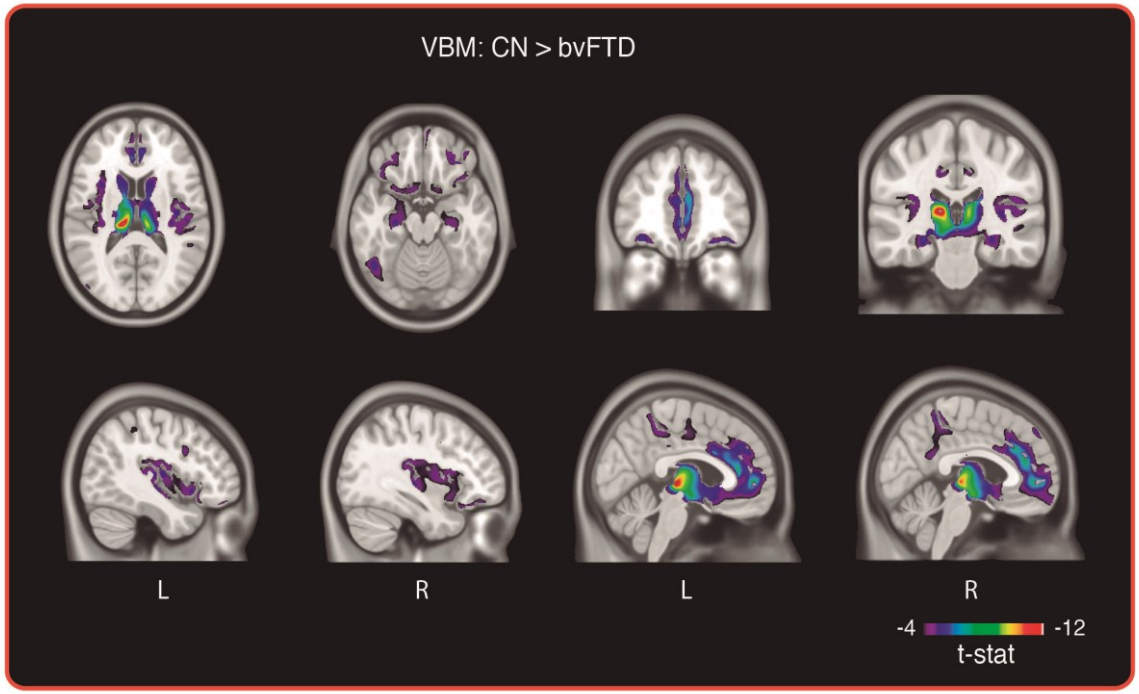

Fig. 5 Overlap (yellow; 22 379 mm^3) between binarized [^{11}C]ABP688 BP_{ND} (red) and [^{18}F]FDG SUV_R (green) t-maps was found with leftward predominance in the in gyrus rectus, anterior cingulate dorso/ventromedial prefrontal cortex, and thalamus. Overlap was also noted with rightward asymmetry in the insula and in the temporal poles bilaterally.

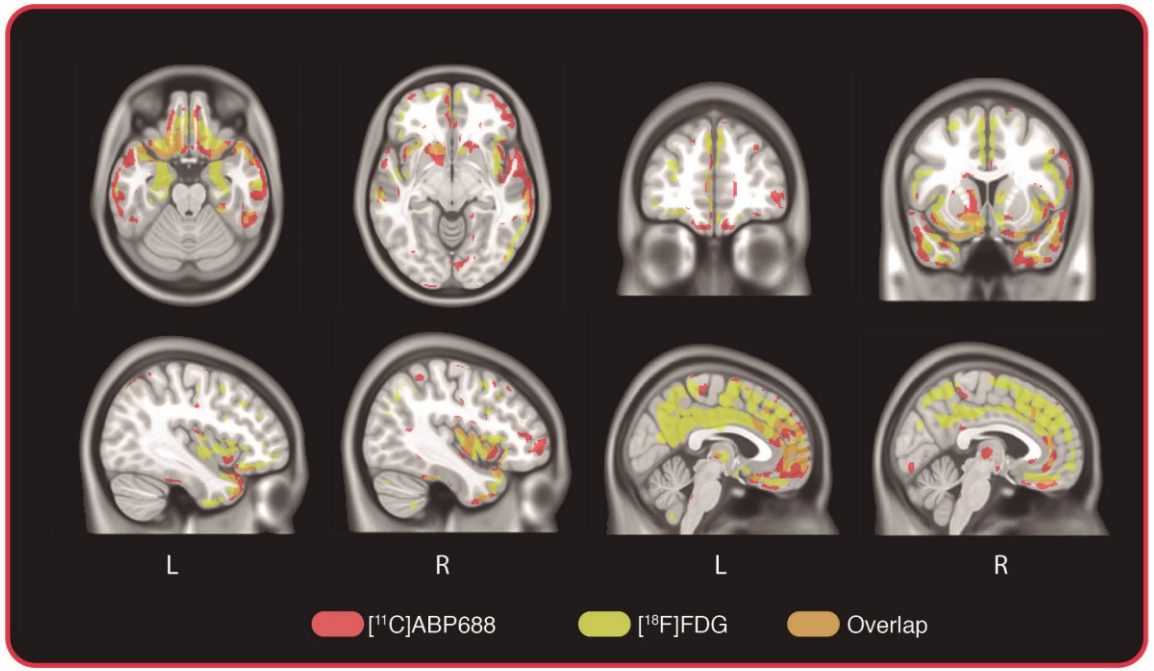

Fig. 6 Overlap (magenta; 13 463mm^3) between binarized [^{11}C]ABP688 BP_{ND} (red) and VBM (purple) t-maps was found with leftward asymmetry in the anterior cingulate, ventromedial prefrontal cortex, thalamus, and head of the caudate nucleus. Rightward asymmetry was noted in the insula and orbitofrontal cortex.

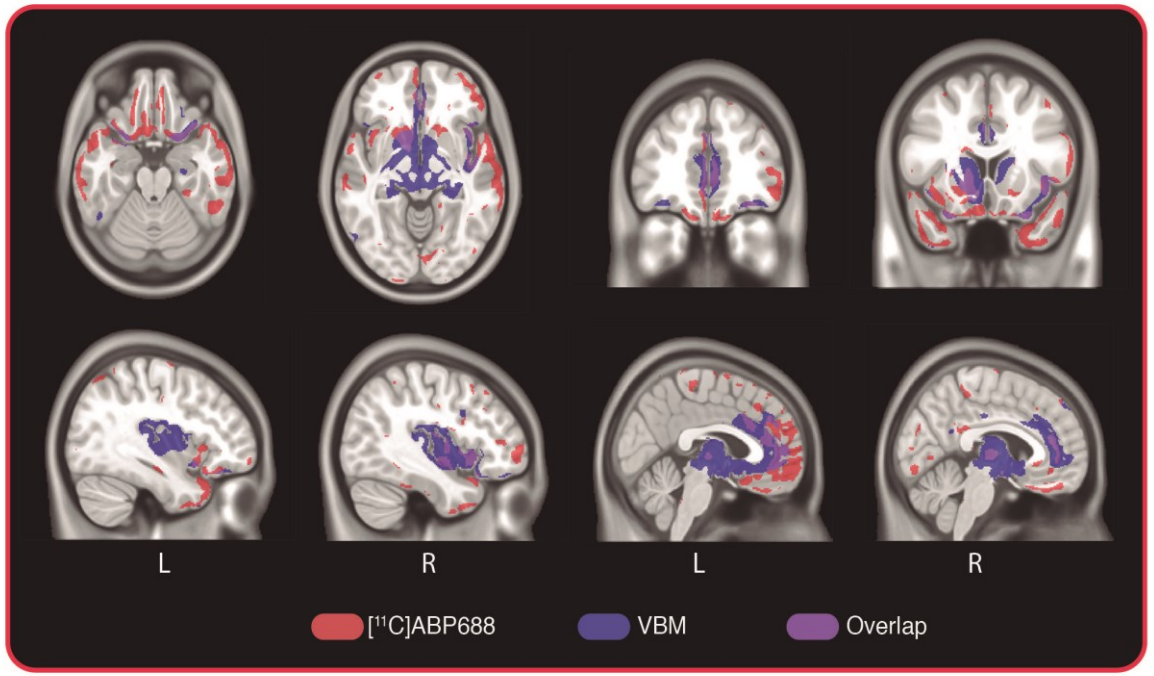

Fig. 7 Overlap (yellow; 14 179mm^3) between binarized [^{18}F]FDG SUV_R (red) and VBM (purple) t-maps was observed with leftward asymmetry in the orbitofrontal cortex, anterior cingulate/ventromedial prefrontal cortex, thalamus and amygdala. Rightward asymmetry was found in the dorsomedial prefrontal cortex, insula, hippocampal formation, and head of the caudate.

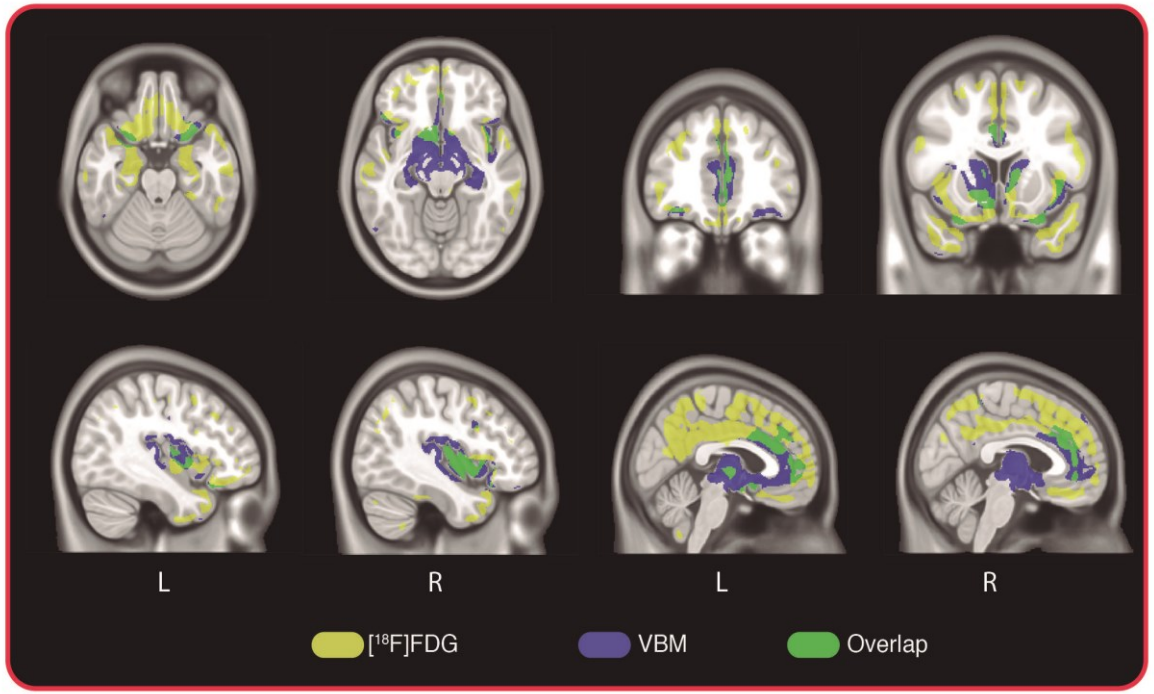

Fig. 8 Subtraction of binarized t-maps ([^{11}C]ABP688 BP_{ND} – [^{18}F]FDG SUV_R – VBM) showed areas characterized only by declines in [^{11}C]ABP688 BP_{ND} (55 742 mm^3). Areas characterized by rightward asymmetry included the inferior temporal lobes, temporal poles gyrus rectus, orbitofrontal cortex, head of the caudate nucleus, posterior cingulate, ventral/dorsolateral prefrontal cortex, lingual gyrus, and occipital cortex. Areas characterized by leftward asymmetry included the putamen, superior temporal lobe, and paracentral lobule.

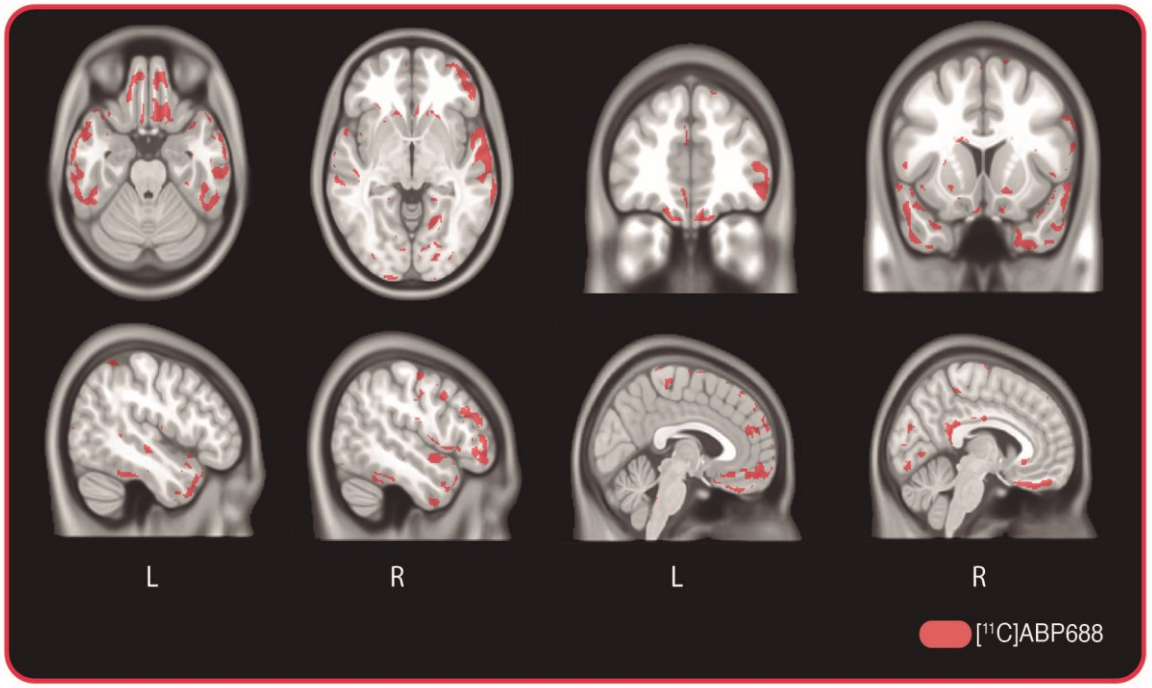

Fig. 9 Subtraction of binarized t-maps ([^{18}F]FDG SUV_R – [^{11}C]ABP688 BP_{ND} – VBM) showed areas characterized only by hypometabolism (86 616 mm^3), including the bilateral insula, medial prefrontal cortex, left posterior paracentral lobule, left frontal operculum, anterior temporal poles, and bilateral cerebellar cortex. Leftward asymmetry was noted for the uncus/amygdalae, parahippocampus, and posterior cingulate/precuneus. Rightward asymmetry was noted for the orbitofrontal gyrus/gyrus rectus.

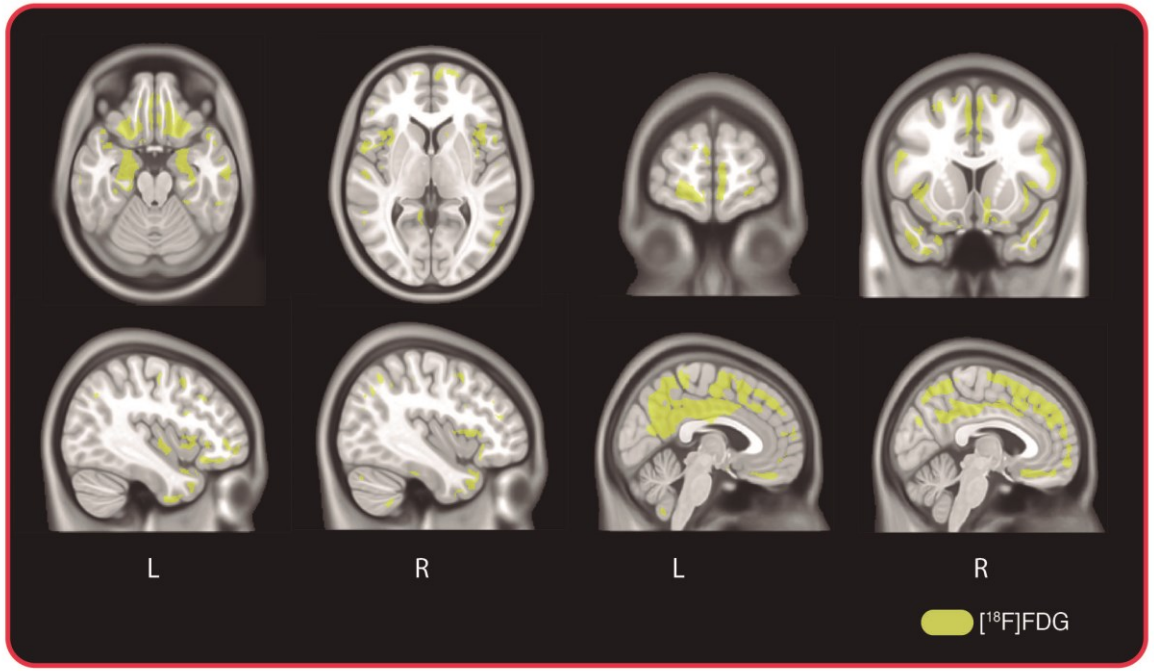

Fig. 10 Subtraction of binarized t-maps (VBM – [^{18}F]FDG SUV_R – [^{11}C]ABP688 BP_{ND}) showed areas characterized only by reductions in GM (67 635 mm^3), including the orbitofrontal gyrus, the right middle temporal gyrus, right temporal operculum, left anterior insula, head of the caudate nucleus bilaterally, left posterior inferior temporal gyrus, the thalamus as well as the posterior portion of the hippocampal formation, bilaterally. Leftward asymmetry was noted for the ventral amygdala, anterior cingulate gyrus, and putamina. Rightward asymmetry was noted for the posterior insula.

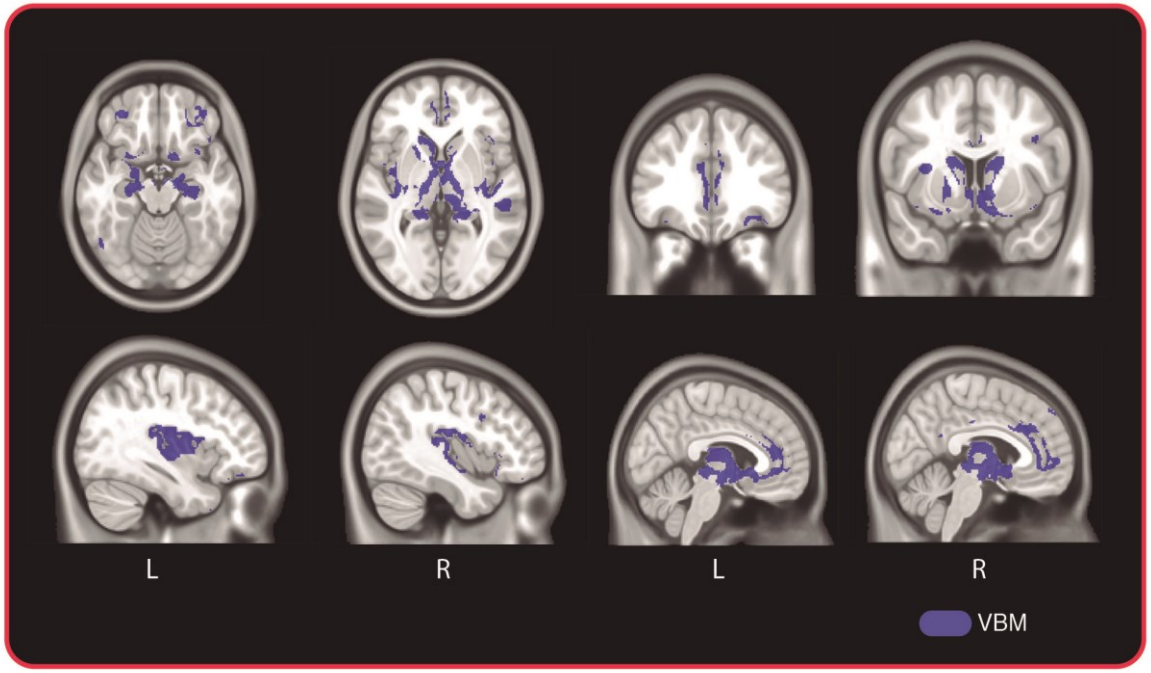

CHAPTER 3: SUMMARY, CONCLUSIONS, AND FUTURE DIRECTIONS

Reduced binding of [^{11}C]ABP688 was found among bvFTD patients in a wide range of brain regions, including the prefrontal cortex, lateral and anterior temporal cortex, basal ganglia, and thalamus. These findings overlapped partially with those for [^{18}F]FDG and VBM, with the volume of tissue affected greatest for impaired metabolism, followed by GM concentrations and mGluR5 availability. Relative to control values, however, reductions were greatest for [^{11}C]ABP688, followed by hypometabolism and GM atrophy. In addition, several areas were characterized only by reduced [^{11}C]ABP688 BP_{ND}, including portions of the gyrus rectus, orbitofrontal gyrus, and occipital cortex.

Our results seemingly refute a previous semi-quantitative immunohistochemistry study in which mGluR5 expression levels were found to be increased in the frontal cortex (Brodmann area 8) of 3 cases with Pick's disease (Dalfo et al. 2005). Since the overexpression of mGluR5 was confined to a subset of cells present in the frontal cortex, this cell specific upregulation may have occurred in the context of declines in mGluR5 availability within the brain as a whole. Alternatively, the difference could be attributable to methodology: while the antibody used in immunohistochemistry binds mGluR5 irrespective of its functional state (i.e. even if the receptor has undergone internalization), availability of the transmembrane allosteric binding site for [^{11}C]ABP688 is dependent on mGluR5 being in its high affinity functional state. In other words, receptor binding results for [^{11}C]ABP688 are dependent on the conformational state of mGluR5 and not, per se, on its level of expression. A change in the proportion of mGluR5 in one or the other affinity state induced by FTLD could thus differentially affect results obtained using these two approaches.

The present study should be interpreted in light of the following considerations. 1) Our sample size was small. This was due, in part, to strict entry criteria: to be eligible for this study, patients were required to meet criteria for probable bvFTD, including both compatible structural and functional neuroimaging findings. Further, they had to be free of motor symptoms and vascular anomalies, and show no signs of amyloid pathology as assessed using [^{11}C]PIB PET. Moreover, healthy controls were required to have a score of 0 on both the NPI and FBI. 2) Our cross-sectional design could not determine whether mGluR5 reductions accompany, precede, or follow neurodegeneration. 3) Although TDP-43 and tau are the most likely underlying pathologies, the absence of genetic and post-mortem data prevents speculation as to the possibly differing associations between FTLD subtypes and patterns of mGluR5 availability. 4) As discussed above, [^{11}C]ABP688 binding can be interpreted as reductions in receptor density or lower affinity for the allosteric binding site. Future *post-mortem* studies are required to disambiguate these two possibilities.

In conclusion, the present study provides the first *in vivo* evidence that bvFTD is characterized by decreased availability of mGluR5, possibly as a result of an abnormal glutamatergic neurotransmission. Moreover, this study represents a proof of concept that PET [^{11}C]ABP688 BP_{ND} can be successfully employed to assess the role of mGluR5 in this population. In addition, this study could carry implications for novel treatment strategies in bvFTD since positive allosteric modulators of mGluR5 function are available and effective in reducing glutamate- and NMDA-induced neuronal cell death (Doria et al. 2013). Future studies are required to substantiate these findings in a larger series, to investigate whether reductions in mGLuR5 represent adaptations or vulnerability to FTLD pathology, and to explore the possibility of mGluR5 based treatment strategies for bvFTD.

References

Alagarsamy S, Rouse ST, Junge C, Hubert GW, Gutman D, Smith Y, Conn PJ (2002) NMDA-induced phosphorylation and regulation of mGluR5 Pharmacology, biochemistry, and behavior 73:299-306

Alagarsamy S, Marino MJ, Rouse ST, Gereau RWt, Heinemann SF, Conn PJ (1999) Activation of NMDA receptors reverses desensitization of mGluR5 in native and recombinant systems Nature neuroscience 2:234-240 doi:10.1038/6338

Alladi S, Xuereb J, Bak T, Nestor P, Knibb J, Patterson K, Hodges JR (2007) Focal cortical presentations of Alzheimer's disease Brain : a journal of neurology 130:2636-2645 doi:10.1093/brain/awm213

Ametamey SM et al. (2007) Human PET studies of metabotropic glutamate receptor subtype 5 with 11C-ABP688 Journal of Nuclear Medicine 48:247-252

Ametamey SM et al. (2006) Radiosynthesis and preclinical evaluation of 11C-ABP688 as a probe for imaging the metabotropic glutamate receptor subtype 5 Journal of nuclear medicine : official publication, Society of Nuclear Medicine 47:698-705

Ango F et al. (2002) Homer-dependent cell surface expression of metabotropic glutamate receptor type 5 in neurons Molecular and cellular neurosciences 20:323-329

Arai T et al. (2006) TDP-43 is a component of ubiquitin-positive tau-negative inclusions in frontotemporal lobar degeneration and amyotrophic lateral sclerosis Biochemical and biophysical research communications 351:602-611 doi:10.1016/j.bbrc.2006.10.093

Ashburner J, Friston KJ (2000) Voxel-based morphometry--the methods NeuroImage 11:805-821 doi:10.1006/nimg.2000.0582

Attucci S, Carla V, Mannaioni G, Moroni F (2001) Activation of type 5 metabotropic glutamate receptors enhances NMDA responses in mice cortical wedges British journal of pharmacology 132:799-806 doi:10.1038/sj.bjp.0703904

Baker M et al. (2006) Mutations in progranulin cause tau-negative frontotemporal dementia linked to chromosome 17 Nature 442:916-919 doi:10.1038/nature05016

Banks SJ, Weintraub S (2009) Generalized and symptom-specific insight in behavioral variant frontotemporal dementia and primary progressive aphasia The Journal of neuropsychiatry and clinical neurosciences 21:299-306 doi:10.1176/appi.neuropsych.21.3.299

Barnes J, Whitwell JL, Frost C, Josephs KA, Rossor M, Fox NC (2006) Measurements of the amygdala and hippocampus in pathologically confirmed Alzheimer disease and frontotemporal lobar degeneration Archives of neurology 63:1434-1439 doi:10.1001/archneur.63.10.1434

Basely M, Ceccaldi M, Boyer L, Mundler O, Guedj E (2013) Distinct patterns of medial temporal impairment in degenerative dementia: a brain SPECT perfusion study in Alzheimer's disease and frontotemporal dementia European journal of nuclear medicine and molecular imaging 40:932-942 doi:10.1007/s00259-013-2389-8

Benquet P, Gee CE, Gerber U (2002) Two distinct signaling pathways upregulate NMDA receptor responses via two distinct metabotropic glutamate receptor subtypes The Journal of neuroscience : the official journal of the Society for Neuroscience 22:9679-9686

Bessis AS, Bertrand HO, Galvez T, De Colle C, Pin JP, Acher F (2000) Three-dimensional model of the extracellular domain of the type 4a metabotropic glutamate receptor: new insights into the activation process Protein science : a publication of the Protein Society 9:2200-2209 doi:10.1110/ps.9.11.2200

Boccardi M et al. (2005) Frontotemporal dementia as a neural system disease Neurobiology of aging 26:37-44 doi:10.1016/j.neurobiolaging.2004.02.019

Borroni B, Agosti C, Bellelli G, Padovani A (2008) Is early-onset clinically different from late-onset frontotemporal dementia? European journal of neurology : the official journal of the European Federation of Neurological Societies 15:1412-1415 doi:10.1111/j.1468-1331.2008.02338.x

Bowie D (2008) Ionotropic glutamate receptors & CNS disorders CNS & neurological disorders drug targets 7:129-143

Brun A, Passant U (1996) Frontal lobe degeneration of non-Alzheimer type. Structural characteristics, diagnostic criteria and relation to other frontotemporal dementias Acta neurologica Scandinavica Supplementum 168:28-30

Brun A, Englund B, Gustafson L, Passant U, Mann DMA, Neary D, Snowden JS (1994) Clinical and neuropathological criteria for frontotemporal dementia. The Lund and Manchester Groups Journal of neurology, neurosurgery, and psychiatry 57:416-418

Brun A (1987) Frontal lobe degeneration of non-Alzheimer type. I. Neuropathology Archives of gerontology and geriatrics 6:193-208

Bunch L, Erichsen MN, Jensen AA (2009) Excitatory amino acid transporters as potential drug targets Expert opinion on therapeutic targets 13:719-731 doi:10.1517/14728220902926127

Cabello N et al. (2009) Metabotropic glutamate type 5, dopamine D2 and adenosine A2a receptors form higher-order oligomers in living cells Journal of neurochemistry 109:1497-1507 doi:10.1111/j.1471-4159.2009.06078.x

Cairns NJ et al. (2007) Neuropathologic diagnostic and nosologic criteria for frontotemporal lobar degeneration: consensus of the Consortium for Frontotemporal Lobar Degeneration Acta neuropathologica 114:5-22 doi:10.1007/s00401-007-0237-2

Cardenas VA, Boxer AL, Chao LL, Gorno-Tempini ML, Miller BL, Weiner MW, Studholme C (2007) Deformation-based morphometry reveals brain atrophy in frontotemporal dementia Archives of neurology 64:873-877 doi:10.1001/archneur.64.6.873

Chiu WZ, Kaat LD, Seelaar H, Rosso SM, Boon AJ, Kamphorst W, van Swieten JC (2010) Survival in progressive supranuclear palsy and frontotemporal dementia Journal of neurology, neurosurgery, and psychiatry 81:441-445 doi:10.1136/jnnp.2009.195719

Conn PJ, Pin JP (1997) Pharmacology and functions of metabotropic glutamate receptors Annual review of pharmacology and toxicology 37:205-237 doi:10.1146/annurev.pharmtox.37.1.205

Costantino G, Macchiarulo A, Pellicciari R (2001) Homology model of the closed, functionally active, form of the amino terminal domain of mGlur1 Bioorganic & medicinal chemistry 9:847-852

Costantino G, Pellicciari R (1996) Homology modeling of metabotropic glutamate receptors. (mGluRs) structural motifs affecting binding modes and pharmacological profile of mGluR1 agonists and competitive antagonists Journal of medicinal chemistry 39:3998-4006 doi:10.1021/jm9601718

Cruts M et al. (2006) Null mutations in progranulin cause ubiquitin-positive frontotemporal dementia linked to chromosome 17q21 Nature 442:920-924 doi:10.1038/nature05017

Cummings JL (1993) Frontal-subcortical circuits and human behavior Archives of neurology 50:873-880

Dalfo E, Albasanz JL, Rodriguez A, Martin M, Ferrer I (2005) Abnormal group I metabotropic glutamate receptor expression and signaling in the frontal cortex in Pick disease Journal of neuropathology and experimental neurology 64:638-647

Davies RR, Scahill VL, Graham A, Williams GB, Graham KS, Hodges JR (2009) Development of an MRI rating scale for multiple brain regions: comparison with volumetrics and with voxel-based morphometry Neuroradiology 51:491-503 doi:10.1007/s00234-009-0521-z

DeJesus-Hernandez M et al. (2011) Expanded GGGGCC hexanucleotide repeat in noncoding region of C9ORF72 causes chromosome 9p-linked FTD and ALS Neuron 72:245-256 doi:10.1016/j.neuron.2011.09.011

Deschwanden A et al. (2011) Reduced metabotropic glutamate receptor 5 density in major depression determined by [(11)C]ABP688 PET and postmortem study The American journal of psychiatry 168:727-734 doi:10.1176/appi.ajp.2011.09111607

Doble A (1999) The role of excitotoxicity in neurodegenerative disease: implications for therapy Pharmacology & therapeutics 81:163-221

Dodd PR (2002) Excited to death: different ways to lose your neurones Biogerontology 3:51-56

Dingledine R, Borges K, Bowie D, Traynelis SF (1999) The glutamate receptor ion channels Pharmacological reviews 51:7-61

Doria JG et al. (2013) Metabotropic glutamate receptor 5 positive allosteric modulators are neuroprotective in a mouse model of Huntington's disease British journal of pharmacology 169:909-921 doi:10.1111/bph.12164

Elmenhorst D et al. (2010) In vivo and in vitro validation of reference tissue models for the mGluR(5) ligand [(11)C]ABP688 Journal of cerebral blood flow and metabolism : official journal of the International Society of Cerebral Blood Flow and Metabolism 30:1538-1549 doi:10.1038/jcbfm.2010.65

Engler H et al. (2008) In vivo amyloid imaging with PET in frontotemporal dementia European journal of nuclear medicine and molecular imaging 35:100-106 doi:10.1007/s00259-007-0523-1

Everett BA et al. (2009) Safety of radial arterial catheterization in PET research subjects Journal of nuclear medicine : official publication, Society of Nuclear Medicine 50:1742 doi:10.2967/jnumed.109.063206

Evers K, Kilander L, Lindau M (2007) Insight in frontotemporal dementia: conceptual analysis and empirical evaluation of the consensus criterion "loss of insight" in frontotemporal dementia Brain and cognition 63:13-23 doi:10.1016/j.bandc.2006.07.001

Ferrer I (1999) Neurons and their dendrites in frontotemporal dementia Dementia and geriatric cognitive disorders 10 Suppl 1:55-60 doi:51214

Focke NK, Trost S, Paulus W, Falkai P, Gruber O (2014) Do manual and voxel-based morphometry measure the same? A proof of concept study Frontiers in psychiatry 5:39 doi:10.3389/fpsyt.2014.00039

Forman MS et al. (2006) Novel ubiquitin neuropathology in frontotemporal dementia with valosin-containing protein gene mutations Journal of neuropathology and experimental neurology 65:571-581

Foster NL, Wilhelmsen K, Sima AA, Jones MZ, D'Amato CJ, Gilman S (1997) Frontotemporal dementia and parkinsonism linked to chromosome 17: a consensus conference. Conference Participants Annals of neurology 41:706-715 doi:10.1002/ana.410410606

Franceschi M et al. (2005) Glucose metabolism and serotonin receptors in the frontotemporal lobe degeneration Annals of neurology 57:216-225 doi:10.1002/ana.20365

Friston KJ, Worsley KJ, Frackowiak RS, Mazziotta JC, Evans AC (1994) Assessing the significance of focal activations using their spatial extent Human brain mapping 1:210-220 doi:10.1002/hbm.460010306

Fukui T, Kertesz A (2000) Volumetric study of lobar atrophy in Pick complex and Alzheimer's disease Journal of the neurological sciences 174:111-121

Galton CJ et al. (2001) Temporal lobe rating scale: application to Alzheimer's disease and frontotemporal dementia Journal of neurology, neurosurgery, and psychiatry 70:165-173

Galton CJ, Patterson K, Xuereb JH, Hodges JR (2000) Atypical and typical presentations of Alzheimer's disease: a clinical, neuropsychological, neuroimaging and pathological study of 13 cases Brain : a journal of neurology 123 Pt 3:484-498

Gass J et al. (2006) Mutations in progranulin are a major cause of ubiquitin-positive frontotemporal lobar degeneration Human molecular genetics 15:2988-3001 doi:10.1093/hmg/ddl241

Genovese CR, Lazar NA, Nichols T (2002) Thresholding of statistical maps in functional neuroimaging using the false discovery rate NeuroImage 15:870-878 doi:10.1006/nimg.2001.1037

Gislason TB, Sjogren M, Larsson L, Skoog I (2003) The prevalence of frontal variant frontotemporal dementia and the frontal lobe syndrome in a population based sample of 85 year olds Journal of neurology, neurosurgery, and psychiatry 74:867-871

Giuliani NR, Calhoun VD, Pearlson GD, Francis A, Buchanan RW (2005) Voxel-based morphometry versus region of interest: a comparison of two methods for analyzing gray matter differences in schizophrenia Schizophrenia research 74:135-147 doi:10.1016/j.schres.2004.08.019

Good CD, Johnsrude IS, Ashburner J, Henson RN, Friston KJ, Frackowiak RS (2001) A voxel-based morphometric study of ageing in 465 normal adult human brains NeuroImage 14:21-36 doi:10.1006/nimg.2001.0786

Goldman JS et al. (2005) Comparison of family histories in FTLD subtypes and related tauopathies Neurology 65:1817-1819 doi:10.1212/01.wnl.0000187068.92184.63

Graham A et al. (2005) Pathologically proven frontotemporal dementia presenting with severe amnesia Brain : a journal of neurology 128:597-605 doi:10.1093/brain/awh348

Gregory CA, Hodges JR (1996) Clinical features of frontal lobe dementia in comparison to Alzheimer's disease Journal of neural transmission Supplementum 47:103-123

Grimmer T, Diehl J, Drzezga A, Forstl H, Kurz A (2004) Region-specific decline of cerebral glucose metabolism in patients with frontotemporal dementia: a prospective 18F-FDG-PET study Dementia and geriatric cognitive disorders 18:32-36 doi:10.1159/000077732

Grootoonk S et al. (2000) Characterization and correction of interpolation effects in the realignment of fMRI time series NeuroImage 11:49-57 doi:10.1006/nimg.1999.0515

Groveman BR, Feng S, Fang XQ, Pflueger M, Lin SX, Bienkiewicz EA, Yu X (2012) The regulation of N-methyl-D-aspartate receptors by Src kinase The FEBS journal 279:20-28 doi:10.1111/j.1742-4658.2011.08413.x

Gunn RN, Lammertsma AA, Hume SP, Cunningham VJ (1997) Parametric imaging of ligand-receptor binding in PET using a simplified reference region model NeuroImage 6:279-287 doi:10.1006/nimg.1997.0303

Gustafson L, Brun A, Passant U (1992) Frontal lobe degeneration of non-Alzheimer type Bailliere's clinical neurology 1:559-582

Gustafson L (1987) Frontal lobe degeneration of non-Alzheimer type. II. Clinical picture and differential diagnosis Archives of gerontology and geriatrics 6:209-223

Harrison PJ, Lyon L, Sartorius LJ, Burnet PW, Lane TA (2008) The group II metabotropic glutamate receptor 3 (mGluR3, mGlu3, GRM3): expression, function and involvement in schizophrenia Journal of psychopharmacology 22:308-322 doi:10.1177/0269881108089818

Harvey RJ, Skelton-Robinson M, Rossor MN (2003) The prevalence and causes of dementia in people under the age of 65 years Journal of neurology, neurosurgery, and psychiatry 74:1206-1209

Hermans E, Challiss RA (2001) Structural, signalling and regulatory properties of the group I metabotropic glutamate receptors: prototypic family C G-protein-coupled receptors The Biochemical journal 359:465-484

Hodges JR et al. (2004) Clinicopathological correlates in frontotemporal dementia Annals of neurology 56:399-406 doi:10.1002/ana.20203

Hodges JR, Davies R, Xuereb J, Kril J, Halliday G (2003) Survival in frontotemporal dementia Neurology 61:349-354

Hodges JR (2001) Frontotemporal dementia (Pick's disease): clinical features and assessment Neurology 56:S6-10

Hodges JR, Patterson K (1996) Nonfluent progressive aphasia and semantic dementia: a comparative neuropsychological study Journal of the International Neuropsychological Society : JINS 2:511-524

Hodges JR, Patterson K, Oxbury S, Funnell E (1992) Semantic dementia. Progressive fluent aphasia with temporal lobe atrophy Brain : a journal of neurology 115 (Pt 6):1783-1806

Hornberger M, Piguet O, Kipps C, Hodges JR (2008) Executive function in progressive and nonprogressive behavioral variant frontotemporal dementia Neurology 71:1481-1488 doi:10.1212/01.wnl.0000334299.72023.c8

Hume SP et al. (1992) Quantitation of carbon-11-labeled raclopride in rat striatum using positron emission tomography Synapse 12:47-54 doi:10.1002/syn.890120106

Hutton M et al. (1998) Association of missense and 5'-splice-site mutations in tau with the inherited dementia FTDP-17 Nature 393:702-705 doi:10.1038/31508

Ikejima C, Yasuno F, Mizukami K, Sasaki M, Tanimukai S, Asada T (2009) Prevalence and causes of early-onset dementia in Japan: a population-based study Stroke; a journal of cerebral circulation 40:2709-2714 doi:10.1161/STROKEAHA.108.542308

Ishii K et al. (1998) Cerebral glucose metabolism in patients with frontotemporal dementia Journal of nuclear medicine : official publication, Society of Nuclear Medicine 39:1875-1878

Jeong Y et al. (2005) 18F-FDG PET findings in frontotemporal dementia: an SPM analysis of 29 patients Journal of nuclear medicine : official publication, Society of Nuclear Medicine 46:233-239

Josephs KA, Hodges JR, Snowden JS, Mackenzie IR, Neumann M, Mann DM, Dickson DW (2011) Neuropathological background of phenotypical variability in frontotemporal dementia Acta neuropathologica 122:137-153 doi:10.1007/s00401-011-0839-6

Josephs KA, Whitwell JL, Parisi JE, Petersen RC, Boeve BF, Jack CR, Jr., Dickson DW (2010) Caudate atrophy on MRI is a characteristic feature of FTLD-FUS European journal of neurology : the official journal of the European Federation of Neurological Societies 17:969-975 doi:10.1111/j.1468-1331.2010.02975.x

Josephs KA, Whitwell JL, Jack CR, Jr. (2008) Anatomic correlates of stereotypies in frontotemporal lobar degeneration Neurobiology of aging 29:1859-1863 doi:10.1016/j.neurobiolaging.2007.04.027

Josephs KA et al. (2006) Clinicopathologic analysis of frontotemporal and corticobasal degenerations and PSP Neurology 66:41-48 doi:10.1212/01.wnl.0000191307.69661.c3

Josephs KA et al. (2006b) Atypical progressive supranuclear palsy with corticospinal tract degeneration Journal of neuropathology and experimental neurology 65:396-405 doi:10.1097/01.jnen.0000218446.38158.61

Josephs KA, Whitwell JL, Jack CR, Parisi JE, Dickson DW (2006c) Frontotemporal lobar degeneration without lobar atrophy Archives of neurology 63:1632-1638 doi:10.1001/archneur.63.11.1632

Johnson JK et al. (2005) Frontotemporal lobar degeneration: demographic characteristics of 353 patients Archives of neurology 62:925-930 doi:10.1001/archneur.62.6.925

Kalia LV, Kalia SK, Salter MW (2008) NMDA receptors in clinical neurology: excitatory times ahead The Lancet Neurology 7:742-755 doi:10.1016/S1474-4422(08)70165-0

Kamo H, McGeer PL, Harrop R, McGeer EG, Calne DB, Martin WR, Pate BD (1987) Positron emission tomography and histopathology in Pick's disease Neurology 37:439-445

Karas GB et al. (2003) A comprehensive study of gray matter loss in patients with Alzheimer's disease using optimized voxel-based morphometry NeuroImage 18:895-907

Karim F, Wang CC, Gereau RWt (2001) Metabotropic glutamate receptor subtypes 1 and 5 are activators of extracellular signal-regulated kinase signaling required for inflammatory pain in mice The Journal of neuroscience : the official journal of the Society for Neuroscience 21:3771-3779

Kertesz A, McMonagle P, Blair M, Davidson W, Munoz DG (2005) The evolution and pathology of frontotemporal dementia Brain : a journal of neurology 128:1996-2005 doi:10.1093/brain/awh598

Khan BK et al. (2012) Atypical, slowly progressive behavioural variant frontotemporal dementia associated with C9ORF72 hexanucleotide expansion Journal of neurology, neurosurgery, and psychiatry 83:358-364 doi:10.1136/jnnp-2011-301883

Kipps CM, Hodges JR, Hornberger M (2010) Nonprogressive behavioural frontotemporal dementia: recent developments and clinical implications of the 'bvFTD phenocopy syndrome' Current opinion in neurology 23:628-632 doi:10.1097/WCO.0b013e3283404309

Kipps CM, Hodges JR, Fryer TD, Nestor PJ (2009) Combined magnetic resonance imaging and positron emission tomography brain imaging in behavioural variant frontotemporal degeneration: refining the clinical phenotype Brain : a journal of neurology 132:2566-2578 doi:10.1093/brain/awp077

Kipps CM, Nestor PJ, Dawson CE, Mitchell J, Hodges JR (2008) Measuring progression in frontotemporal dementia: implications for therapeutic interventions Neurology 70:2046-2052 doi:10.1212/01.wnl.0000313366.76973.8a

Kipps CM, Nestor PJ, Fryer TD, Hodges JR (2007) Behavioural variant frontotemporal dementia: not all it seems? Neurocase 13:237-247 doi:10.1080/13554790701594870

Kunishima N et al. (2000) Structural basis of glutamate recognition by a dimeric metabotropic glutamate receptor Nature 407:971-977 doi:10.1038/35039564

Kwiatkowski TJ, Jr. et al. (2009) Mutations in the FUS/TLS gene on chromosome 16 cause familial amyotrophic lateral sclerosis Science 323:1205-1208 doi:10.1126/science.1166066

Lammertsma AA, Hume SP (1996) Simplified reference tissue model for PET receptor studies NeuroImage 4:153-158 doi:10.1006/nimg.1996.0066

Lammertsma AA, Bench CJ, Hume SP, Osman S, Gunn K, Brooks DJ, Frackowiak RS (1996b) Comparison of methods for analysis of clinical [11C]raclopride studies Journal of cerebral blood flow and metabolism: official journal of the International Society of Cerebral Blood Flow and Metabolism 16:42-52 doi:10.1097/00004647-199601000-00005

Le Ber I et al. (2006) Demographic, neurological and behavioural characteristics and brain perfusion SPECT in frontal variant of frontotemporal dementia Brain: a journal of neurology 129:3051-3065 doi:10.1093/brain/awl288

Lodge D (2009) The history of the pharmacology and cloning of ionotropic glutamate receptors and the development of idiosyncratic nomenclature Neuropharmacology 56:6-21 doi:10.1016/j.neuropharm.2008.08.006

Liguz-Lecznar M, Skangiel-Kramska J (2007) Vesicular glutamate transporters (VGLUTs): the three musketeers of glutamatergic system Acta neurobiologiae experimentalis 67:207-218

Lipton SA (2006) Paradigm shift in neuroprotection by NMDA receptor blockade: memantine and beyond Nature reviews Drug discovery 5:160-170 doi:10.1038/nrd1958

Liu W et al. (2004) Behavioral disorders in the frontal and temporal variants of frontotemporal dementia Neurology 62:742-748

Lough S, Kipps CM, Treise C, Watson P, Blair JR, Hodges JR (2006) Social reasoning, emotion and empathy in frontotemporal dementia Neuropsychologia 44:950-958 doi:10.1016/j.neuropsychologia.2005.08.009

Luccini E, Musante V, Neri E, Brambilla Bas M, Severi P, Raiteri M, Pittaluga A (2007) Functional interactions between presynaptic NMDA receptors and metabotropic glutamate receptors co-expressed on rat and human noradrenergic terminals British journal of pharmacology 151:1087-1094 doi:10.1038/sj.bjp.0707280

Mackenzie IR et al. (2010) Nomenclature and nosology for neuropathologic subtypes of frontotemporal lobar degeneration: an update Acta neuropathologica 119:1-4 doi:10.1007/s00401-009-0612-2

Mackenzie IR et al. (2009) Nomenclature for neuropathologic subtypes of frontotemporal lobar degeneration: consensus recommendations Acta neuropathologica 117:15-18 doi:10.1007/s00401-008-0460-5

Manes F (2012) Psychiatric conditions that can mimic early behavioral variant frontotemporal dementia: the importance of the new diagnostic criteria Current psychiatry reports 14:450-452 doi:10.1007/s11920-012-0294-7

Manes FF, Torralva T, Roca M, Gleichgerrcht E, Bekinschtein TA, Hodges JR (2010) Frontotemporal dementia presenting as pathological gambling Nature reviews Neurology 6:347-352 doi:10.1038/nrneurol.2010.34

Massimo L et al. (2009) Neuroanatomy of apathy and disinhibition in frontotemporal lobar degeneration Dementia and geriatric cognitive disorders 27:96-104 doi:10.1159/000194658

Masu M, Tanabe Y, Tsuchida K, Shigemoto R, Nakanishi S (1991) Sequence and expression of a metabotropic glutamate receptor Nature 349:760-765 doi:10.1038/349760a0

McKhann GM, Albert MS, Grossman M, Miller B, Dickson D, Trojanowski JQ (2001) Clinical and pathological diagnosis of frontotemporal dementia: report of the Work Group on Frontotemporal Dementia and Pick's Disease Archives of neurology 58:1803-1809

Mendez MF, Lauterbach EC, Sampson SM, Research ACo (2008) An evidence-based review of the psychopathology of frontotemporal dementia: a report of the ANPA Committee on Research The Journal of neuropsychiatry and clinical neurosciences 20:130-149 doi:10.1176/appi.neuropsych.20.2.130

Mendez MF, Shapira JS, McMurtray A, Licht E, Miller BL (2007) Accuracy of the clinical evaluation for frontotemporal dementia Archives of neurology 64:830-835 doi:10.1001/archneur.64.6.830

Mendez MF, Shapira JS, Miller BL (2005) Stereotypical movements and frontotemporal dementia Movement disorders: official journal of the Movement Disorder Society 20:742-745 doi:10.1002/mds.20465

Mendez M, Bagerta, BA, Edwards-lee, T (1997) Self-injurious behavior in frontotemporal dementia Neurocase: The Neural Basis of Cognition 3:213-136

Mendez MF, Foti DJ (1997b) Lethal hyperoral behaviour from the Kluver-Bucy syndrome Journal of neurology, neurosurgery, and psychiatry 62:293-294

Mesulam MM (1982) Slowly progressive aphasia without generalized dementia Annals of neurology 11:592-598 doi:10.1002/ana.410110607

Mioshi E, Kipps CM, Hodges JR (2009) Activities of daily living in behavioral variant frontotemporal dementia: differences in caregiver and performance-based assessments Alzheimer disease and associated disorders 23:70-76

Mioshi E, Hodges JR (2009b) Rate of change of functional abilities in frontotemporal dementia Dementia and geriatric cognitive disorders 28:419-426 doi:10.1159/000255652

Neary D et al. (1998) Frontotemporal lobar degeneration: a consensus on clinical diagnostic criteria Neurology 51:1546-1554

Neary D, Snowden JS, Northen B, Goulding P (1988) Dementia of frontal lobe type Journal of neurology, neurosurgery, and psychiatry 51:353-361

Neary D et al. (1987) Single photon emission tomography using 99mTc-HM-PAO in the investigation of dementia Journal of neurology, neurosurgery, and psychiatry 50:1101-1109

Neumann M et al. (2007) TDP-43 in the ubiquitin pathology of frontotemporal dementia with VCP gene mutations Journal of neuropathology and experimental neurology 66:152-157 doi:10.1097/nen.0b013e31803020b9

Neumann M et al. (2006) Ubiquitinated TDP-43 in frontotemporal lobar degeneration and amyotrophic lateral sclerosis Science 314:130-133 doi:10.1126/science.1134108

Niswender CM, Conn PJ (2010) Metabotropic glutamate receptors: physiology, pharmacology, and disease Annual review of pharmacology and toxicology 50:295-322 doi:10.1146/annurev.pharmtox.011008.145533

Olney JW, Neurotoxicity of excitatory amino acids, in: E.G. McGeer, J.W. Olney, P.L. McGeer (Eds.), Kainic Acid as a Tool in Neurobiology, Raven Press, New York, 1978, pp. 95–121.

Pan PL et al. (2012) Gray matter atrophy in behavioral variant frontotemporal dementia: a meta-analysis of voxel-based morphometry studies Dementia and geriatric cognitive disorders 33:141-148 doi:10.1159/000338176

Passant U, Elfgren C, Englund E, Gustafson L (2005) Psychiatric symptoms and their psychosocial consequences in frontotemporal dementia Alzheimer disease and associated disorders 19 Suppl 1:S15-18

Perry RJ, Miller BL (2001) Behavior and treatment in frontotemporal dementia Neurology 56:S46-51

Piguet O, Hornberger M, Mioshi E, Hodges JR (2011) Behavioural-variant frontotemporal dementia: diagnosis, clinical staging, and management The Lancet Neurology 10:162-172 doi:10.1016/S1474-4422(10)70299-4

Piguet O, Hornberger M, Shelley BP, Kipps CM, Hodges JR (2009) Sensitivity of current criteria for the diagnosis of behavioral variant frontotemporal dementia Neurology 72:732-737 doi:10.1212/01.wnl.0000343004.98599.45

Pin JP, Duvoisin R (1995) The metabotropic glutamate receptors: structure and functions Neuropharmacology 34:1-26

Postiglione A et al. (2008) Fronto-temporal dementia presenting as Geschwind's syndrome Neurocase 14:264-270 doi:10.1080/13554790802269976

Procter AW, Qurne M, Francis PT (1999) Neurochemical features of frontotemporal dementia Dementia and geriatric cognitive disorders 10 Suppl 1:80-84 doi:51219

Rabinovici GD, Rascovsky K, Miller BL (2008) Frontotemporal lobar degeneration: clinical and pathologic overview Handbook of clinical neurology 89:343-364 doi:10.1016/S0072-9752(07)01233-X

Rabinovici GD et al. (2007) 11C-PIB PET imaging in Alzheimer disease and frontotemporal lobar degeneration Neurology 68:1205-1212 doi:10.1212/01.wnl.0000259035.98480.ed

Rabinovici GD et al. (2007b) Distinct MRI atrophy patterns in autopsy-proven Alzheimer's disease and frontotemporal lobar degeneration American journal of Alzheimer's disease and other dementias 22:474-488 doi:10.1177/1533317507308779

Rankin KP, Kramer JH, Miller BL (2005) Patterns of cognitive and emotional empathy in frontotemporal lobar degeneration Cognitive and behavioral neurology : official journal of the Society for Behavioral and Cognitive Neurology 18:28-36

Rascovsky K et al. (2011) Sensitivity of revised diagnostic criteria for the behavioural variant of frontotemporal dementia Brain: a journal of neurology 134:2456-2477 doi:10.1093/brain/awr179

Rascovsky K et al. (2007) Diagnostic criteria for the behavioral variant of frontotemporal dementia (bvFTD): current limitations and future directions Alzheimer disease and associated disorders 21:S14-18 doi:10.1097/WAD.0b013e31815c3445

Rascovsky K et al. (2005) Rate of progression differs in frontotemporal dementia and Alzheimer disease Neurology 65:397-403 doi:10.1212/01.wnl.0000171343.43314.6e

Ratnavalli E, Brayne C, Dawson K, Hodges JR (2002) The prevalence of frontotemporal dementia Neurology 58:1615-1621

Renton AE et al. (2011) A hexanucleotide repeat expansion in C9ORF72 is the cause of chromosome 9p21-linked ALS-FTD Neuron 72:257-268 doi:10.1016/j.neuron.2011.09.010

Roberson ED et al. (2005) Frontotemporal dementia progresses to death faster than Alzheimer disease Neurology 65:719-725 doi:10.1212/01.wnl.0000173837.82820.9f

Romano C, Yang WL, O'Malley KL (1996) Metabotropic glutamate receptor 5 is a disulfide-linked dimer The Journal of biological chemistry 271:28612-28616

Romano C, Sesma MA, McDonald CT, O'Malley K, Van den Pol AN, Olney JW (1995) Distribution of metabotropic glutamate receptor mGluR5 immunoreactivity in rat brain The Journal of comparative neurology 355:455-469 doi:10.1002/cne.903550310

Rosen HJ et al. (2004) Neuropsychological and functional measures of severity in Alzheimer disease, frontotemporal dementia, and semantic dementia Alzheimer disease and associated disorders 18:202-207

Rosso SM et al. (2003) Frontotemporal dementia in The Netherlands: patient characteristics and prevalence estimates from a population-based study Brain: a journal of neurology 126:2016-2022 doi:10.1093/brain/awg204

Rothstein JD (1996) Excitotoxicity hypothesis Neurology 47:S19-25; discussion S26

Riedl L, Mackenzie IR, Forstl H, Kurz A, Diehl-Schmid J (2014) Frontotemporal lobar degeneration: current perspectives Neuropsychiatric disease and treatment 10:297-310 doi:10.2147/NDT.S38706

Rinne JO, Laine M, Kaasinen V, Norvasuo-Heila MK, Nagren K, Helenius H (2002) Striatal dopamine transporter and extrapyramidal symptoms in frontotemporal dementia Neurology 58:1489-1493

Roberson ED et al. (2005) Frontotemporal dementia progresses to death faster than Alzheimer disease Neurology 65:719-725 doi:10.1212/01.wnl.0000173837.82820.9f

Rohrer JD et al. (2009) The heritability and genetics of frontotemporal lobar degeneration Neurology 73:1451-1456 doi:10.1212/WNL.0b013e3181bf997a

Rosen HJ et al. (2002) Patterns of brain atrophy in frontotemporal dementia and semantic dementia Neurology 58:198-208

Rosso SM et al. (2003) Frontotemporal dementia in The Netherlands: patient characteristics and prevalence estimates from a population-based study Brain: a journal of neurology 126:2016-2022 doi:10.1093/brain/awg204

Rothstein JD (1995) Excitotoxic mechanisms in the pathogenesis of amyotrophic lateral sclerosis Advances in neurology 68:7-20; discussion 21-27

Rowe CC et al. (2007) Imaging beta-amyloid burden in aging and dementia Neurology 68:1718-1725 doi:10.1212/01.wnl.0000261919.22630.ea

Salmond CH, Ashburner J, Vargha-Khadem F, Connelly A, Gadian DG, Friston KJ (2002) Distributional assumptions in voxel-based morphometry NeuroImage 17:1027-1030

Schaeffer E, Duplantier A (2010) Glutamate and Neurodegenerative Disease. In: Dominguez C (ed) Neurodegnerative Diseases. Springer-Verlag Berlin Heidelberg, Heidelberg, pp 91-147

Sedaghat F et al. (2007) Evaluation of dopaminergic function in frontotemporal dementia using I-FP-CIT single photon emission computed tomography Neuro-degenerative diseases 4:382-385 doi:10.1159/000105159

Seelaar H et al. (2010) Frequency of ubiquitin and FUS-positive, TDP-43-negative frontotemporal lobar degeneration Journal of neurology 257:747-753 doi:10.1007/s00415-009-5404-z

Seelaar H et al. (2008) Distinct genetic forms of frontotemporal dementia Neurology 71:1220-1226 doi:10.1212/01.wnl.0000319702.37497.72

Seeley WW, Crawford R, Rascovsky K, Kramer JH, Weiner M, Miller BL, Gorno-Tempini ML (2008) Frontal paralimbic network atrophy in very mild behavioral variant frontotemporal dementia Archives of neurology 65:249-255 doi:10.1001/archneurol.2007.38

Shaw PJ (1994) Excitotoxicity and motor neurone disease: a review of the evidence Journal of the neurological sciences 124 Suppl:6-13

Shi J et al. (2005) Histopathological changes underlying frontotemporal lobar degeneration with clinicopathological correlation Acta neuropathologica 110:501-512 doi:10.1007/s00401-005-1079-4

Shinagawa S et al. (2008) Cognitive function and psychiatric symptoms in early- and late-onset frontotemporal dementia Dementia and geriatric cognitive disorders 25:439-444 doi:10.1159/000124751

Skibinski G et al. (2005) Mutations in the endosomal ESCRTIII-complex subunit CHMP2B in frontotemporal dementia Nature genetics 37:806-808 doi:10.1038/ng1609

Snowden JS et al. (2011) The most common type of FTLD-FUS (aFTLD-U) is associated with a distinct clinical form of frontotemporal dementia but is not related to mutations in the FUS gene Acta neuropathologica 122:99-110 doi:10.1007/s00401-011-0816-0

Snowden J, Neary D, Mann D (2007) Frontotemporal lobar degeneration: clinical and pathological relationships Acta neuropathologica 114:31-38 doi:10.1007/s00401-007-0236-3

Snowden JS, Bathgate D, Varma A, Blackshaw A, Gibbons ZC, Neary D (2001) Distinct behavioural profiles in frontotemporal dementia and semantic dementia Journal of neurology, neurosurgery, and psychiatry 70:323-332

Snowden JS (1999) Semantic dysfunction in frontotemporal lobar degeneration Dementia and geriatric cognitive disorders 10 Suppl 1:33-36 doi:51209

Sperfeld AD et al. (1999) FTDP-17: an early-onset phenotype with parkinsonism and epileptic seizures caused by a novel mutation Annals of neurology 46:708-715

Spooren W, Ballard T, Gasparini F, Amalric M, Mutel V, Schreiber R (2003) Insight into the function of Group I and Group II metabotropic glutamate (mGlu) receptors: behavioural characterization and implications for the treatment of CNS disorders Behavioural pharmacology 14:257-277 doi:10.1097/01.fbp.0000081783.35927.8f

Sreedharan J et al. (2008) TDP-43 mutations in familial and sporadic amyotrophic lateral sclerosis Science 319:1668-1672 doi:10.1126/science.1154584

Sturm VE, Ascher EA, Miller BL, Levenson RW (2008) Diminished self-conscious emotional responding in frontotemporal lobar degeneration patients Emotion 8:861-869 doi:10.1037/a0013765

Swartz J, Miller B, Lesser I, Booth R, Darby A, Wohl M, Benson D (1997) Behavioral phenomenology in Alzheimer's disease, frontotemporal dementia, and late-life depression: a retrospective analysis. J Geriatr Psychiatry Neurol 10:67-74

Talbot PR, Lloyd JJ, Snowden JS, Neary D, Testa HJ (1998) A clinical role for 99mTc-HMPAO SPECT in the investigation of dementia? Journal of neurology, neurosurgery, and psychiatry 64:306-313

Thomas U (2002) Modulation of synaptic signalling complexes by Homer proteins Journal of neurochemistry 81:407-413

Treyer V et al. (2008) Radiation dosimetry and biodistribution of 11C-ABP688 measured in healthy volunteers European journal of nuclear medicine and molecular imaging 35:766-770 doi:10.1007/s00259-007-0638-4

Treyer V et al. (2007) Evaluation of the metabotropic glutamate receptor subtype 5 using PET and 11C-ABP688: assessment of methods Journal of nuclear medicine: official publication, Society of Nuclear Medicine 48:1207-1215 doi:10.2967/jnumed.107.039578

Vance C et al. (2009) Mutations in FUS, an RNA processing protein, cause familial amyotrophic lateral sclerosis type 6 Science 323:1208-1211 doi:10.1126/science.1165942

Vardy E, Langheinrich, T, Hinz, R, Snowden, J, Gerhard, A, Richardson, A, Neary, D, Anton, J, Brown, G, Herholz, K (2010) Journal of neurology, neurosurgery, and psychiatry doi:10.1136/jnnp.2010.226340.114

Varma AR et al. (2002) Diagnostic patterns of regional atrophy on MRI and regional cerebral blood flow change on SPECT in young onset patients with Alzheimer's disease,

frontotemporal dementia and vascular dementia Acta neurologica Scandinavica 105:261-269

Varma AR, Snowden JS, Lloyd JJ, Talbot PR, Mann DM, Neary D (1999) Evaluation of the NINCDS-ADRDA criteria in the differentiation of Alzheimer's disease and frontotemporal dementia Journal of neurology, neurosurgery, and psychiatry 66:184-188

Warwick HK, Nahorski SR, Challiss RA (2005) Group I metabotropic glutamate receptors, mGlu1a and mGlu5a, couple to cyclic AMP response element binding protein (CREB) through a common Ca2+ - and protein kinase C-dependent pathway Journal of neurochemistry 93:232-245 doi:10.1111/j.1471-4159.2005.03012.x

Watts GD et al. (2004) Inclusion body myopathy associated with Paget disease of bone and frontotemporal dementia is caused by mutant valosin-containing protein Nature genetics 36:377-381 doi:10.1038/ng1332

Whitwell JL (2009) Voxel-based morphometry: an automated technique for assessing structural changes in the brain The Journal of neuroscience: the official journal of the Society for Neuroscience 29:9661-9664 doi:10.1523/JNEUROSCI.2160-09.2009

Whitwell JL et al. (2009b) Voxel-based morphometry patterns of atrophy in FTLD with mutations in MAPT or PGRN Neurology 72:813-820 doi:10.1212/01.wnl.0000343851.46573.67

Whitwell JL, Josephs KA (2007) Voxel-based morphometry and its application to movement disorders Parkinsonism & related disorders 13 Suppl 3:S406-416 doi:10.1016/S1353-8020(08)70039-7

Whitwell JL, Jack CR, Jr., Senjem ML, Josephs KA (2006) Patterns of atrophy in pathologically confirmed FTLD with and without motor neuron degeneration Neurology 66:102-104 doi:10.1212/01.wnl.0000191395.69438.12

Whitwell JL, Sampson EL, Watt HC, Harvey RJ, Rossor MN, Fox NC (2005) A volumetric magnetic resonance imaging study of the amygdala in frontotemporal lobar degeneration and Alzheimer's disease Dementia and geriatric cognitive disorders 20:238-244 doi:10.1159/000087343

Whitwell JL, Jack CR, Jr. (2005b) Comparisons between Alzheimer disease, frontotemporal lobar degeneration, and normal aging with brain mapping Topics in magnetic resonance imaging : TMRI 16:409-425 doi:10.1097/01.rmr.0000245457.98029.e1

Whitwell JL et al. (2005c) Magnetic resonance imaging signatures of tissue pathology in frontotemporal dementia Archives of neurology 62:1402-1408 doi:10.1001/archneur.62.9.1402

Woolley JD, Gorno-Tempini ML, Seeley WW, Rankin K, Lee SS, Matthews BR, Miller BL (2007) Binge eating is associated with right orbitofrontal-insular-striatal atrophy in frontotemporal dementia Neurology 69:1424-1433 doi:10.1212/01.wnl.0000277461.06713.23

Womack KB et al. (2011) Temporoparietal hypometabolism in frontotemporal lobar degeneration and associated imaging diagnostic errors Archives of neurology 68:329-337 doi:10.1001/archneurol.2010.295

Yang Y, Schmitt HP (2001) Frontotemporal dementia: evidence for impairment of ascending serotoninergic but not noradrenergic innervation. Immunocytochemical and quantitative study using a graph method Acta neuropathologica 101:256-270